Back-Arc Spreading Systems

Geological, Biological, Chemical, and Physical Interactions

David M. Christie, Charles R. Fisher,
Sang-Mook Lee, and Sharon Givens
Editors

AGU

Modes of Crustal Accretion in Back-Arc Basins: Inferences From the Lau Basin

Fernando Martinez and Brian Taylor

School of Ocean and Earth Science and Technology, University of Hawaii at Manoa, Honolulu, Hawaii, USA

As island arc rifting evolves to mature back-arc spreading, the nature of melt generation and mode of crustal accretion may vary in response to the interplay of different subduction-related processes and conditions, including (1) changes in mantle dynamics from flux-melting and buoyancy-driven upwelling at the arc volcanic front to decompression melting driven by plate separation at back-arc spreading centers; (2) re-circulation of refractory material through arc and back-arc melting regimes by mantle wedge corner flow; (3) changes in the locus of magmatic centers relative to the arc volcanic front; (4) variable locus of initial rifting and breakup; (5) spatially varying rheology attributable to mantle wedge hydration gradients with distance from the slab; (6) slab subduction rate, dip, and length. We discuss the possible influence of these factors on crustal accretion processes in light of observations from intra-oceanic back-arc basins, with particular focus on new compilations of swath bathymetry and sidescan imagery from the Lau Basin. In the Lau Basin south of 18°S, the active spreading centers undergo large changes in morphology and crustal characteristics as they separate from the arc volcanic front. Ahead of the southern limit of organized seafloor spreading, a broad area of high acoustic backscatter indicates a wide, "distributed" form of crustal accretion. Parts of the western Lau Basin have been previously interpreted as remnants of a tectonically rifted preexisting arc. The swath mapping data show, however, that western basin morphology is similar to that formed by the sites of currently active magmatic crustal accretion to the east. These observations support a revised model of Lau Basin evolution in which essentially the entire back-arc basin is formed by magmatic crustal accretion, but crustal thickness and morphology reflect the changing locus of the magmatic centers with respect to a mantle wedge of varying chemical fertility and rheology. Compared to mid-ocean settings, the observations imply an expanded range of crustal accretion variables in arc-proximal magmatic centers in which seafloor morphology is more indicative of mantle wedge chemistry than spreading rate.

1. INTRODUCTION

Back-arc basins are sites of extension and crustal accretion genetically related to subduction zones [*Weissel*, 1981] where water, sediments, crust, and mantle lithosphere are cycled back into the Earth [*Stern*, 2002]. The subducted lithosphere releases water into the overlying mantle wedge through metamorphic breakdown of hydrated minerals at a range of depths down to ~150–200 km [*Schmidt and Poli*, 1998]. A consequence of the resulting mantle hydration is flux melting of the mantle wedge and the formation of island and submarine arc volcanoes that are a characteristic feature of subduction settings. Arc volcanism can extend into the back-arc but typically has an abrupt

Back-Arc Spreading Systems: Geological, Biological, Chemical, and Physical Interactions
Geophysical Monograph Series 166

10.1029/166GM03

trenchward limit and maximum subparallel to the trench, which forms a chain of arc volcanoes known as the arc volcanic front (AVF) [*Tatsumi*, 1986; *Tatsumi and Eggins*, 1995]. *Karig* [1970], using geophysical data from the Lau Basin, first proposed that back-arc basins form by rifting of arc massifs followed by crustal accretion between the separating conjugate rifted arc margins. *Molnar and Atwater* [1978] argued that the volcanic arc should be a favored site of the initial rifting as it represents a weak zone maintained by arc volcanism—a locus of heat, melt, and locally thickened crust, all of which reduce lithospheric strength [*Kusznir and Park*, 1987]. Observations of rifting in arc and back-arc systems show that this prediction is approximately correct, the initial sites of rifting occurring within ±50 km of the volcanic arc [*Taylor and Karner*, 1983]. A related prediction of this model is that the chemistry of lavas should change in time from arc-like to mid-ocean ridge basalt (MORB)-like with increasing basin opening and separation of the magmatic centers from the line of arc volcanoes [e.g., *Hawkins and Melchior*, 1985]. Significant effort has been devoted to examining subduction effects on back-arc geochemistry, but the effects on geophysical and structural characteristics of crustal accretion have received comparatively less consideration.

In this paper we first discuss various processes that may affect back-arc crustal accretion, focusing on effects that are genetically related to active subduction zones. We thus limit discussion of slab edge or "tear" effects [e.g., *Govers and Wortel*, 2005; *Livermore*, this volume], where exterior mantle may flow laterally into the mantle wedge and produce effects that may be more related to the nature of the exterior mantle [e.g., *Portnyagin et al.*, 2005] than to generic subduction processes. For similar reasons we do not discuss the well-mapped back-arc spreading centers of the North Fiji Basin, where large anomalous mantle thermal effects far from the active subduction zones are inferred to dominate spreading characteristics [*Lagabrielle et al.*, 1997]. We also do not directly address complex subduction environments such as in the Bismarck Sea [e.g., *Lee and Ruellan*, this volume], where a long history of multiple active and paleo subduction zones may have broadly influenced the mantle wedge in ways not simply related to the present-day subduction setting.

After reviewing subduction processes, we describe the morphologic and geophysical characteristics of the Lau Basin, focusing on new bathymetric and sonar imagery compilations from south of ~18°S. In this area the present spreading geometry and kinematics are well constrained and the spreading centers systematically approach the AVF, allowing the effect of arc proximity on spreading characteristics to be examined. We show that the identified active spreading centers are consistent with narrow plate boundary zones of crustal accretion, like mid-ocean ridges (MORs) [e.g., *Taylor et al.*, 1996], but display unusual morphologic and crustal characteristics with abrupt transitions. At the southern end of the spreading systems and very near the AVF, however, the mode of extension changes into a broader area of high acoustic backscatter, which appears to be a less focused form of magmatic crustal accretion. We hypothesize that slow basin opening rates, arc proximity, and high rates of mantle hydration from the slab in this area lead to a weak rheology, enabling a broader plate boundary zone than at the spreading axes to the north.

We then examine the western margin of the basin, which has been interpreted as a broad area of arc rifting. We show instead that the characteristics of this area are consistent with the patterns of magmatic crustal accretion to the east. From these observations we propose a revised interpretation of the evolution of the Lau Basin. Rather than a broadly distributed rift phase, the margins of the Lau Basin reflect magmatic crustal accretion processes with morphologic variations similar to those that occur along the active neovolcanic zones. Taken together, the morphology and mode of crustal accretion in the basin appear to be an expression of the evolving locus of the magmatic centers with respect to a mantle wedge of variable composition and rheology.

2. PROCESSES AFFECTING MAGMA GENERATION IN BACK-ARC BASINS

We discuss various models, effects, and observations related to magma generation and crustal accretion in back-arc basins. Some of these models are long-held hypotheses; others are extrapolations of observations from mid-ocean settings; a few are speculations based on physical principles and deductions that have not been directly investigated in this setting. Our intent is to take a broad view on possible mechanisms, from a largely geophysical perspective, as a prelude to examine if and how these concepts may be applied to the geophysical and morphologic observations from the Lau Basin.

2.1. Early Geochemical and Magmatic Evolution of Back-Arc Basins and Mantle Wedge Dynamics

The model of arc rifting followed by back-arc spreading predicts that as back-arc basins form and widen, magmatic centers should initially be coincident with or close to the arc magma source and then progressively separate from it. This implies a shift in the composition of magma, from an initial strong arc-influence toward MORB-like compositions [*Tarney et al.*, 1977; *Saunders and Tarney*, 1979; *Hawkins and Melchior*, 1985; *Gribble et al.*, 1998]. Efforts to test this hypothesis have motivated extensive sampling in back-arc basins, including drilling in the Lau Basin, the Mariana Trough, and the Izu-Bonin Arc. Consistent conclusions have nevertheless been hindered by several effects. Sampling of back-arc lavas shows extreme geochemical variability with arc-like and MORB-like samples sometimes in close proximity [*Volpe*

et al., 1990; *Hawkins and Allan*, 1994]. Back-arc basins can have complex tectonic histories with rift jumps and spreading center propagation events [*Parson et al.*, 1990], confounding models of a simple progressive evolutionary development. Further, sampling of lavas from different back-arc tectonic settings has led to some opposing findings: Sampling of the early Izu-Bonin interarc rift lavas showed them to be much more like the back-arc basin basalts (BABBs) that characterize mature basins rather than arc-like [*Fryer et al.*, 1990; *Hochstaedter et al.*, 1990a]. From these observations *Fryer et al.* [1990] concluded that "the model of a progressive change in back-arc basin basalt composition from arc-like to mid-ocean ridge-like, as a function of the evolution of the basin...is not generally applicable". Yet analysis of samples from the arc-proximal northern Mariana Trough magmatic axis compared with the more evolved central Mariana Trough "supports general models for back-arc basin evolution whereby early back-arc basin basalts have a strong arc component which diminishes in importance relative to MORB as the back-arc basin widens" [*Stern, et al.*, 1990; see also *Gribble et al.*, 1998].

Recent geophysical observations and numerical modeling suggest a possible resolution of these conflicting geochemical findings. Three-dimensional tomographic imaging [*Tamura et al.*, 2002; *Hasegawa and Nakajima*, 2004] of the mantle wedge beneath the Japan Arc shows sheet-like low-velocity regions above the slab that locally thicken and have lower velocities in bands transverse to the arc. The thicker and lower velocity regions in the mantle wedge correspond to geologically and geophysically imaged "hot-finger" zones [*Tamura et al.*, 2002], interpreted as localized regions of magma genesis, ascent, and emplacement extending from the back-arc to the AVF. Tomographic profiles transverse to the arc along volcanic gaps show much weaker or absent seismic velocity anomalies [*Tamura et al.*, 2002]. These observations give some support to early ideas of buoyancy-driven diapiric mantle wedge processes in arc volcanism [*Marsh*, 1979] but modify this model to include up-dip transport in the mantle wedge above and subparallel to the slab [*Hasegawa and Nakajima*, 2004]. Three-dimensional numerical modeling reproduces some of the tomographic features, including discrete slab-parallel convective rolls in the mantle wedge, but requires low mantle viscosities [*Honda and Yoshida*, 2005]. These models and geophysical observations of mantle wedge dynamics are consistent with the surface geologic and geochemical observations of spaced arc volcanoes with intervening areas of mantle much less affected by slab-derived magmas and fluids. Thus, lavas from early rifts located behind and between arc volcanoes (like the Sumisu and Torishima Rifts of the Izu-Bonin arc [*Fryer et al.*, 1990; *Hochstaedter et al.*, 1990a, 1990b]) may be derived from mantle relatively uncontaminated by slab-induced melting, compared with the spaced loci of the arc magmas themselves (see Figure 1). This "initial" state may be only slightly modified during early arc rifting, but with continued basin opening, mantle wedge flow

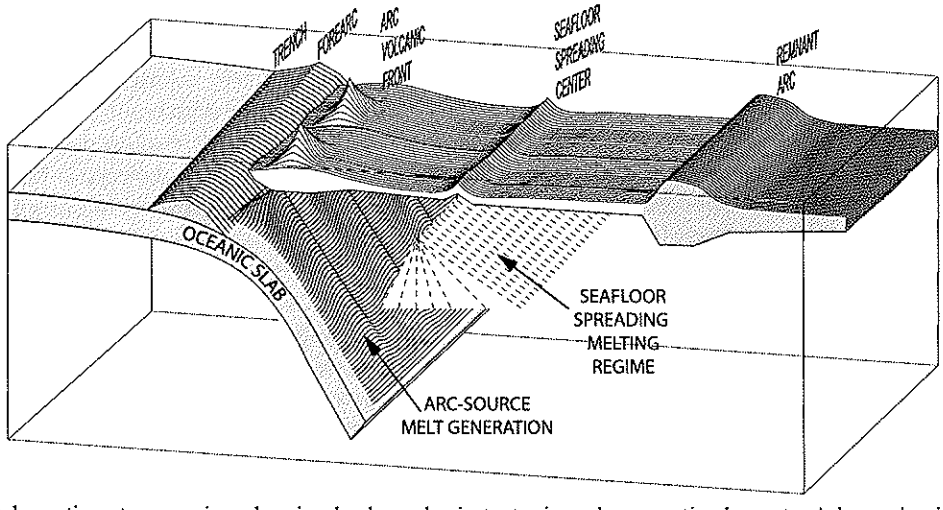

Figure 1. Schematic cut-away view showing back-arc basin tectonic and magmatic elements. A low seismic velocity zone observed above and subparallel to the slab is thought to result from water released from the slab, leading to flux melting in the mantle wedge [*Hasegawa and Nakajima*, 2004]. This zone is thicker and shows lower velocities in arc-transverse bands or "hot fingers" terminating beneath arc volcanoes [*Tamura et al.*, 2002]. The spaced arc-transverse hot fingers are interpreted as the primary loci of arc melt supply to the arc volcanic front. In contrast, mature back-arc ridge magmatism is driven by plate separation in the overriding plate, leading to mantle advection and pressure-release melting in triangular melting regimes. During early back-arc basin formation and when spreading centers are near the arc volcanic front, the arc and back-arc melt generation processes interact to various extents.

patterns should progressively change. Rifting implies rupture and separation of the overriding lithosphere into two plates, which will cause mantle flow to evolve from three-dimensional buoyantly driven "hot fingers" that supply arc volcanism to the more two-dimensional advective patterns of seafloor spreading systems driven by surface plate separation [e.g., *Reid and Jackson*, 1981; *Phipps Morgan and Forsyth*, 1988]. Seismic observations indicate that in cross-section, seafloor spreading mantle melting regimes form triangular regions hundreds of kilometers wide at solidus depths [*MELT Seismic Team*, 1998]. Such plate-driven advective flow patterns can thus entrain large volumes of mantle over a much broader region than does the more localized buoyancy-driven systems that may supply AVF volcanism (Figure 1). The degree of interaction between seafloor spreading and AVF mantle flow patterns will probably vary with the locus of initial rifting and breakup (see below) and other parameters such as slab dip, length, and subduction rate. Large-scale differences in mantle dynamics may, however, account for the discordant observations of a broad and systematic geochemical evolution that *is* observed along active spreading axes (e.g,, Mariana Tough [*Stern et al.*, 1990; *Gribble et al.*, 1998] and Lau Basin [*Pearce et al.*, 1995]) but *is not* seen in early-stage interarc rifts (e.g., Izu-Bonin arc [*Fryer et al.*, 1990; *Hochstaedter et al.*, 1990a, 1990b]).

Entrainment of large volumes of mantle in back-arc seafloor spreading melting regimes does not necessarily lead to melt homogenization even after organized spreading is well established, and geochemical heterogeneity on the scale of samples only 10s of meters apart continues to complicate the interpretation of magmatic processes [*Volpe et al.*, 1990; *Hawkins and Allan*, 1994]. At a larger scale, however, features such as seafloor depth, gravity anomalies, and, where available, seismic crustal thickness measurements reflect the integrated melt production that we suggest is tied to bulk changes in mantle composition within the melting regime. Geochemical support for this inference is found in the few back-arc locations where, despite significant chemical heterogeneity, dense sampling resolves systematic geochemical changes that show correlation with large scale (10s of km) bathymetric features [*Volpe et al.*, 1990]. Seafloor morphology and acoustic backscatter characteristics can thus not only help identify the geologic nature (volcanic or tectonic) of seafloor features but also have implications for mantle chemistry and melting processes.

2.2. Arc Proximity and Effects of Rift Jumps, Propagation, and Asymmetric Back-Arc Accretion

Arc proximity affects the magmatic productivity, morphology, and chemical nature of back-arc spreading centers. This effect has been noted in the Mariana and Manus basins [*Gribble et al.*, 1996; *Martinez and Taylor*, 2003; *Yamazaki et al.*, 2003] and East Scotia Ridge [*Livermore et al.*, 1997; *Taylor and Martinez*, 2003] but is perhaps best documented in the Lau Basin, where spreading centers (the Central and Eastern Lau Spreading Center, see below) are positioned progressively between ~40–180 km from the AVF [*Jenner et al.*, 1987; *Vallier et al.*, 1991; *Wiedicke and Collier*, 1993; *Pearce et al.*, 1995; *Martinez and Taylor*, 2002]. Along these systems, thick andesitic crust and shallow peaked axial high morphology near the AVF change abruptly to deeper and faulted axes with thinner than normal oceanic crust and finally to more MOR-like characteristics with increasing separation from the AVF. These effects have been attributed to variations in mantle wedge melt productivity because of high water content (which lowers mantle solidus temperatures) in mantle near the AVF, less hydrous but refractory mantle farther from the AVF, and essentially anhydrous MORB-source mantle underlying spreading centers when sufficiently far (>170 km in the case of the Lau Basin) from the AVF [*Martinez and Taylor*, 2002] (Figure 2). Therefore the position of the magmatic centers with respect to the AVF can be an important parameter controlling the spatial variations in composition, crustal thickness, and morphology of the basin [*Martinez et al.*, 2006].

Although back-arc opening may eventually isolate back-arc basin magmatic centers from those of the AVF, this need not take place symmetrically or progressively. Back-arc magmatic centers can migrate asymmetrically, with basin opening tending to remain near the AVF. Thus, a large fraction of back-arc basin crust may be influenced by the arc-proximal magmatic stage even after 100s of km of basin opening. A prominent example is the southernmost Mariana Trough where a magmatically robust spreading axis [*Martinez et al.*, 2000] has remained adjacent to the AVF [*Fryer et al.*, 1998] producing anomalously shallow seafloor depths across all of this part of the basin. In the central Mariana Trough, where the spreading axis is virtually indistinguishable morphologically from MOR spreading [*Kong et al.*, 1992; *Kong*, 1993], active accretion occurs two to three times faster on the western flank [*Deschamps and Fujiwara*, 2003]. Asymmetric spreading appears to increase northward as the magmatic axis approaches the AVF once more [*Martinez et al.*, 1995; *Yamazaki and Murakami*, 1998; *Yamazaki et al.*, 2003]. Other examples of asymmetric back-arc crustal accretion include the Havre Trough [*Wright*, 1993; *Wright et al.*, 1996] and the Taupo volcanic zone in New Zealand [*Stern*, 1987]. In addition to this type of essentially continuous asymmetric accretion or migration of magmatic centers, discrete jumps or propagation events also occur that transfer magmatic centers discontinuously toward or away from the AVF. In the Lau Basin, the Eastern Lau spreading center propagates toward the AVF at its southern end while being replaced by southward propagation of the more arc-distal Central Lau spreading center from the

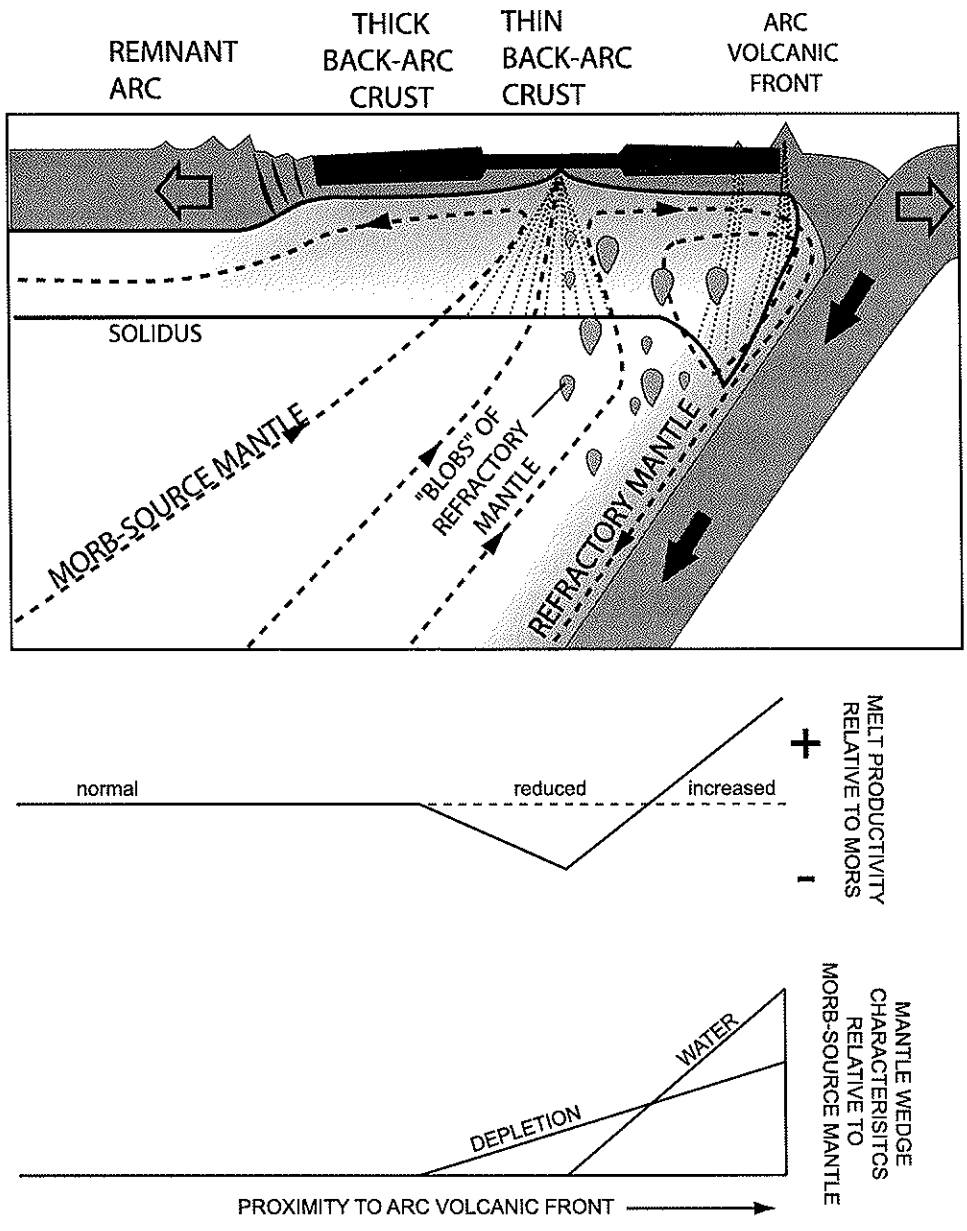

Figure 2. Corner flow effects on back-arc melting. Slab-driven corner flow circulates residual mantle beneath the back-arc basin. Buoyant residual mantle is rehydrated by water released from the slab, becomes less viscous, and rises into the melting regime of back-arc spreading center as discrete diapirs or "blobs". These residual mantle diapirs have been stripped of incompatible elements by prior melt extraction and are also less fertile than the ambient MORB-source mantle. They decrease melt production at the spreading center by volumetrically displacing more fertile (MORB-source) mantle within the melting regime while contributing little melt or trace elements themselves. Most of the resulting lavas therefore are sourced largely from normal degrees of melting of MORB-source mantle and appear to have little geochemical evidence of depletion, although the resulting crustal thicknesses are considerably thinner than normal. A few highly depleted lavas, resulting from small volumes of melt from the refractory mantle blobs, are sometimes sampled (e.g., samples from dredges D23–25 in the N-ELSC [*Pearce et al.*, 1995]). Back-arc melting near the arc volcanic front takes place in a hydrous environment, where a significantly lowered solidus generates high extents of melting and therefore thick crust despite higher levels of depletion. Bottom curves schematically show depletion and hydration trends observed in the mantle wedge and their hypothesized effects on spreading center melt productivity with distance from the volcanic front.

north [*Parson et al.*, 1990]. At the Fonualei Rift and spreading center [*Zellmer and Taylor*, 2001] in the northern Lau Basin, a rifting and spreading system is propagating southward into the northern Tofua arc. These various forms of asymmetric crustal accretion can introduce arc-like melts and anomalous topographic effects even in wide and mature back-arc basins by moving the magmatic centers closer to the magmatic arc. Thus, back-arc basins may not systematically evolve towards MOR-like conditions with time and degree of opening, and may display various modes at different locations within the same basin.

2.3. Tectonic Setting of Initial Rifting and Breakup

Although rifting of arc systems is roughly centered on the AVF, as predicted by *Molnar and Atwater* [1978], the specific site of rupture may vary [*Taylor and Karner*, 1983]. Rifting or breakup can occur dominantly in the back-arc (e.g., Izu-Bonin Arc [*Taylor*, 1992]), centered along the arc itself (e.g., Mariana Trough [*Stern et al.*, 1984]), or in the forearc (e.g., Lau Basin [*Hawkins and Allan*, 1994]) (Figure 3). The locus of rifting may also change along a single rift system, such as in the Izu-Bonin arc, where the rifts surround the AVF at 29°N [*Taylor*, 1992], or in the Vanuatu arc, where the rift locations migrate from the back-arc to the forearc south of Anatom [*Maillet, et al.*, 1995]. The varying sites of initial rupture of the arc massif imply different degrees of disruption of the arc edifices and their magmatic conduits. The source of arc magma, however, is tied to the deeper subducting slab and mantle wedge and has a characteristic locus of eruption, the AVF. As long as subduction continues, arc magma generation processes in the deeper mantle (hydration and flux melting) should also continue, despite disruption of the overriding arc lithosphere. With rifting, breakup, and separation of the arc lithospheric flanks, a second source of melting develops, the result of passive mantle upwelling and decompression melting, as at mid-ocean ridges. The varying locus of overriding plate breakup with respect to the AVF therefore affects how these two melt-generating processes spatially and temporally evolve and interact (see Figure 3).

When rifting and breakup occur behind the AVF, the arc volcanoes remain with the forearc plate and the back-arc basin develops behind the arc. This locus of rifting and breakup minimizes the interaction between arc and back-arc magmatic processes because arc volcanoes and deeper conduits may not be highly disrupted; subsequent evolution will typically involve an increasing separation of arc and back-arc sources of melt. The extinct Parece Vela and Shikoku Basins rifted towards the rear of the arc: the Palau-Kyushu Ridge is a narrow (few 10s of km) remnant arc with few distinct vestiges of arc or rear-arc volcanic edifices, especially adjacent to the Parece Vela basin [*Kobayashi et al.*, 1995; *Okino et al.*, 1998; *Nishizawa et al.*, 2005]. Most of the original Eocene-Oligocene arc/forearc, estimated to have been originally over 300 km wide [*Taylor*, 1992], was not disrupted. The western margins of the Parece Vela and Shikoku back-arc basins show an abrupt faulted breakup that transitions rapidly eastward into oceanic-type seafloor spreading fabric and has well-delineated abyssal hills and magnetic anomalies [*Kobayashi et al.*, 1995; *Okino et al.*, 1998; *Nishizawa et al.*, 2005].

When rifting and breakup occur along the AVF, subaerial arc volcanism may largely cease when the arc volcanic edifices are tectonically disrupted, but arc-type magmas may continue to erupt at smaller submarine seamounts or back-arc spreading centers near the expected locus of the AVF above the slab (e.g., [*Fryer et al.*, 1998; *Gribble et al.*, 1998; *Martinez et al.*, 2000]). As the back-arc magmatic centers separate from the locus of the AVF, the volcanic edifices will rebuild. This may be the case in the Mariana Trough, where the original arc volcanoes were disrupted by rifting [*Hussong and Uyeda*, 1981; *Bloomer et al.*, 1989]. Stratovolcanoes have been rebuilt at the Central Island Province, where the back-arc spreading axis is most separated from the AVF, but arc edifices become progressively smaller and submarine at the Northern and Southern Seamount Provinces, where the back-arc axis approaches the AVF [*Dixon and Stern*, 1983; *Stern et al.*, 1988; *Bloomer et al.*, 1989]. Breakup that is focused along the AVF thus predicts greater interactions between arc magmatic sources to at least the early stages of back-arc development than where rifting and breakup occur rearward of the AVF.

If rifting occurs in the forearc, the nascent back-arc basin is in an inverted tectonic position with respect to the active arc and will be associated with an unusually broad remnant arc. This appears to be the case in the Lau Basin [*Hawkins*, 1994], where Lau Ridge (Korobasaga Group) arc volcanism (now part of the remnant arc) occurred up to 4 million years (4.5–2.2 Ma) [*Whelan et al.*, 1985] after the basin began to open in the forearc at ~6 Ma. The present tectonic geometry, with the active Tofua arc now trenchward of the back-arc basin, indicates that the arc system had to reinitiate, migrate, or step across the widening basin. Cores recovered during ODP Leg 135 showed evidence that volcaniclastic sediments, interpreted as derived from proximal intrabasin arc sources, migrated west to east with basin opening [*Bednarz and Schmincke*, 1994; *Clift and Dixon*, 1994; *Parson et al.*, 1994]. These volcaniclastic sediments may thus represent the eastward migration of arc magmatism across the widening Lau Basin. Arc magmatism eventually stabilized at the eastern edge of the back-arc basin, where the construction of modern Tofua arc volcanoes is estimated to have progressed southward over the last 3 million years, becoming a robust system since only ~1 Ma [*Tappin et al.*, 1994; *Hawkins*, 1995b].

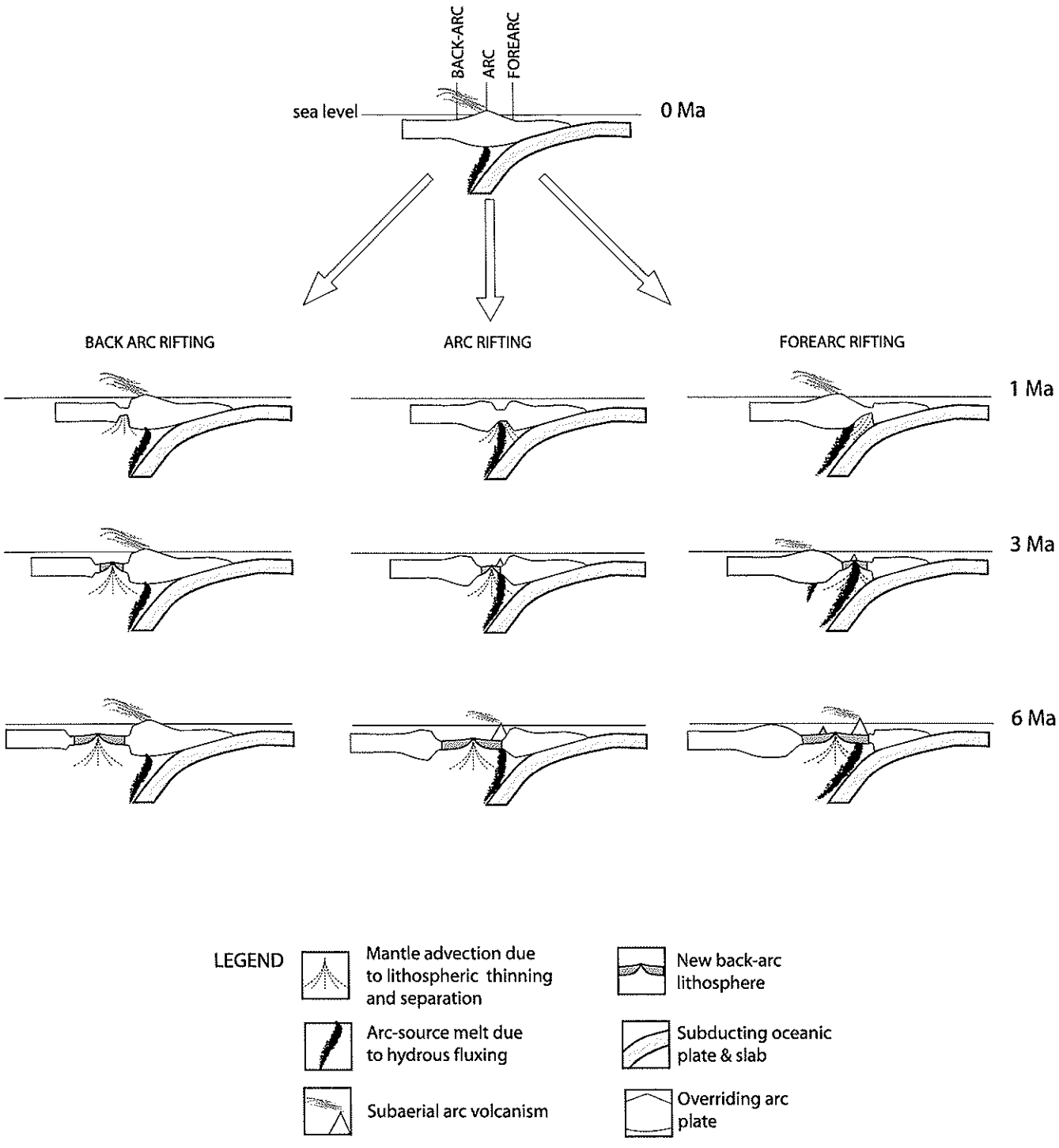

Figure 3. Variable location of arc massif rifting and breakup and hypothesized development of the geometry of arc and back-arc magma genesis. The initial slab and arc lithospheric geometry is shown on top. The three panels below schematically show the temporal development of rifting and back-arc spreading centered at back-arc, arc, and forearc settings. The panels depict the different geometry and interaction with increasing back-arc opening between arc melt sources (tied to the subducting slab) and back-arc melt generation (tied to mantle advection driven by thinning and separation of the overriding lithospheric plates).

Thus, forearc rifting and breakup may involve the greatest degree of interaction between back-arc and arc magmatism. The remnant arc edifices are, for the most part, not tectonically disrupted and may remain active for a time during early basin opening. The arc magma source, however, which is tied to the slab, migrates trenchward relative to the developing back-arc basin, locally introducing arc volcanism across the largely BABB magmatism of the back-arc [*Hawkins*, 1995a]. Once the arc magma source has migrated across the zones of active extension in the back-arc and underlies tectonically stable forearc plate, the AVF can reestablish itself. Thus, when the breakup of the arc massif occurs in the forearc, as in the Lau Basin, the sources of arc and back-arc volcanism first undergo a relative migration *across* each other within the developing basin. This transposition stage of arc and back-arc magmatic sources may lead to greater morphologic and petrologic heterogeneity within the affected part of the basin, compared to cases where breakup is at the AVF or to the rear of the arc and where the development typically involves a progressive separation of these magmatic sources.

2.4. Rheology of the Mantle Wedge

As a consequence of introducing water from the breakdown of hydrous minerals in the slab [*Schmidt and Poli*, 1998], mantle wedge rheology may spatially vary. Mineral physics experiments show that water has a large effect on the strength of olivine, the dominant constituent of the upper mantle [*Hirth and Kohlstedt*, 1996; *Karato and Jung*, 1998]. Generally low viscosity in the mantle wedge is predicted from modeling gravity, geoid, and topography of back-arc regions [*Billen and Gurnis*, 2001; *Billen et al.*, 2003]. A low-viscosity mantle wedge decouples the sinking slab from the overriding lithosphere, which would otherwise be pulled down by the sinking slab (by several km) [*Billen and Gurnis*, 2001]. Analyses of BABB [*Garcia et al.*, 1979; *Sinton and Fryer*, 1987; *Muenow et al.*, 1991; *Stolper and Newman*, 1994; *Gribble et al.*, 1996, 1998] show that back-arc lavas have significantly higher water contents than MORB and that water concentrations increase toward the AVF.

These observations have implications for the formation of the narrow plate boundary zones [*Macdonald*, 1982] that characterize seafloor spreading systems and for the focusing of melt to the axis. Because of the incompatibility of water in mantle minerals, it has been argued that mantle melting and melt extraction at MORs will strongly dehydrate the residual mantle and thereby greatly increase its strength relative to fertile (MORB-source) mantle [*Hirth and Kohlstedt*, 1996; *Phipps Morgan*, 1997; *Karato and Jung*, 1998]. Thus, the process of melt formation and extraction at a spreading center may generate a strong "compositional" lithosphere [*Phipps Morgan*, 1997] not directly related to its temperature structure as in classical models of the "thermal" lithosphere [e.g., *Parsons and Sclater*, 1977]. Magnetotelluric experiments [*Evans et al.*, 2005] have imaged the conductivity structure beneath the East Pacific Rise axis and interpreted a low-conductivity layer that lies shallower than about 60 km as being the dehydrated upper mantle residual to melt extraction at the ridge. A similar depth (68 km) boundary has been inferred in the central Pacific lithosphere from teleseismic anisotropy studies [*Gaherty et al.*, 1996]; this is also interpreted to delimit dehydrated upper mantle from more hydrous, undepleted mantle beneath. Thus the narrow plate boundary zones observed at MORs may be enabled by melting and dehydration, which thereby strengthens the residual mantle near the axis to a far greater degree than predicted by purely thermal models [*Hirth and Kohlstedt*, 1996]. It has also been proposed [*Hirth and Kohlstedt*, 1996; *Phipps Morgan*, 1997] that the strengthening of the near-axis lithosphere by this mechanism can focus melt to the spreading center. *Spiegelman and McKenzie* [1987] showed that pressure gradients generated by the flow and deformation of the sub-axial mantle matrix can focus melt to the spreading center if the shear viscosity is sufficiently high (~10^{21} Pa s). Although it initially appeared that the required viscosities were too high for this mechanism to pertain to spreading centers [*Scott and Stevenson*, 1989], subsequent analysis suggests that dehydrated residual mantle may have sufficiently high viscosity [*Hirth and Kohlstedt*, 1996; *Phipps Morgan*, 1997].

These findings and inferences from MOR studies have interesting implications for crustal accretion in back-arc environments of various hydrous contents. Although speculative, it could be argued that high rates of water injection from the slab into the mantle wedge near the AVF counteract the dehydration effects of mantle melt extraction, especially at slow spreading rates, when melt production rates may also be low. If so, and if mantle dehydration by melt extraction is critical to the formation of a narrow plate boundary zone, then wider than normal plate boundary zones may be enabled by rehydration of mantle and lithosphere in parts of back-arc basins by slab-derived fluids. New observations from the Lau back-arc basin (see Section 4 below) suggest this may occur within back-arc extensional zones near the AVF.

2.5. Mantle Wedge Corner Flow

Virtually all models of mantle dynamics beneath back-arc basins predict viscous coupling between the mantle and the subducting slab leading to wedge corner flow. Corner flow dynamics have been considered largely in terms of their effects on AVF chemistry, although a few modeling studies explored effects on back-arc magmatism [*Ribe*, 1989; *Conder et al.*, 2002]. Depletions of high-field-strength elements

(HFSE) such as Ta, Nb, Zr, and heavy rare-earth elements (HREE) are characteristic of AVF lavas. The observation that the depletions increase toward the AVF has been explained by previous melt extraction from the arc source mantle (at a back-arc spreading center or in rear-arc volcanism) and flow of the residual mantle toward the AVF, where it undergoes additional melting [*Ewart and Hawkesworth*, 1987; *McCulloch and Gamble*, 1991; *Woodhead et al.*, 1993; *Hochstaedter et al.*, 2000; *Stern et al.*, 2006]. The observation that the depletions do not increase with time has been cited as geochemical evidence of mantle wedge convection [*Hochstaedter et al.*, 2000]. Thus the models and observations suggest a convecting system in which ambient (MORB-source) mantle is increasingly depleted in HREE by melting processes behind the arc as it flows towards the wedge corner, whereas fluid mobile elements are added from the slab [e.g., *Hochstaedter et al.*, 2001]. With flux melting and melt extraction, the residual mantle becomes more buoyant (from the extraction of iron) and stronger (from dehydration) [*Phipps Morgan*, 1997] and is passively carried away from beneath the AVF by viscous coupling with slab motion. The downward advection of this residual mantle with the slab will create an unstable situation, however. It has been proposed that the gravitational instability of downward advection of residual mantle can modulate or reverse wedge corner flow [e.g., *Davies and Stevenson*, 1992]. A more likely alternative, however, is that the buoyant residual mantle will become rehydrated by water released from the slab, decrease in viscosity, and rise into the mantle wedge interior. These diapirs of refractory residual mantle may then become entrained in the melting regimes of back-arc spreading centers and significantly affect melt production (Figure 2). Observational support for this idea comes from crustal thickness measurements at back-arc ridges and flanking seafloor. In the Lau Basin the Eastern Lau spreading center (ELSC) crust thins from 9 [*Turner et al.*, 1999] to 5.5 km northward along its length, whereas crustal thicknesses of ~7–8 km characterize the Central Lau spreading center (CLSC) [*Crawford et al.*, 2003]. Because water is predicted to increase mantle melting [*Stolper and Newman*, 1994], its increasing concentrations toward the arc [*Pearce et al.*, 1995] should only lead to increasing crustal thickness from the observed normal values near the CLSC (~7 km) to thicker than normal (9 km) at the VFR. Thinner than normal (5.5 km) crust near the northern ELSC, however, cannot be simply explained by variations in water contents. The observation that samples from the northern ELSC appear to be more depleted than those of the CLSC [*Pearce et al.*, 1995] suggests that the thinner than normal crust may be explained by the entrainment of refractory mantle (having undergone previous melting) into the melting regime of the northern ELSC, but not into that of the more arc-distal CLSC. The entrainment of highly refractory "blobs" of mantle into a melting regime together with ambient (MORB-source) mantle would decrease the total volume of melt produced at the spreading center, because the refractory component would contribute much less melt but volumetrically displace MORB-source mantle, which would melt normally to produce MORB-like lavas (Figure 2). Thus, most samples would not appear highly depleted even though crust is thinner than normal, but occasionally some highly depleted lavas from the more refractory "blobs" would be sampled [e.g., *Pearce et al.*, 1995].

2.6. Slab Length, Dip, and Subduction Rate

The overriding and subducting lithospheres physically delimit the mantle wedge; it has been proposed that they control melting column thickness and thereby affect melt production [e.g., *Plank and Langmuir*, 1988]. Viscous coupling of the mantle wedge with the slab suggests that subduction rate will control the rate of corner flow in the wedge. Corner flow brings fertile mantle into the zone of hydrous fluxing and maintains nearly steady depletion levels in arc volcanism that would otherwise become more depleted with time [*Hochstaedter et al.*, 2000]. Near-the-wedge-corner modeling suggests that the upper plate lithosphere can be thermally thinned by corner flow, leading to a component of upward flow and decompression melting [*Conder et al.*, 2002]. Tomographic imaging shows low-velocity zones above the slab that are interpreted as source regions of arc magmas [*Tamura et al.*, 2002; *Hasegawa and Nakajima*, 2004]. Therefore the dip and length of the slab may control the extent to which these arc components can be introduced beneath back-arc basins. As previously discussed, corner flow also may remove refractory material from the wedge corner and recirculate it beneath the back-arc. Thus slabs that extend far behind the arc and subduct relatively quickly, as in the Tonga subduction zone, may be more effective in transporting this material beneath back-arc magmatic centers than more slowly subducting and steeply dipping slabs as in the central Mariana Trough [*Chiu et al.*, 1991; *Gudmundsson and Sambridge*, 1998]. Subduction rate may also affect mantle wedge temperatures. Numerical modeling [*Ribe*, 1989; *Peacock*, 1996] indicates that increasing subduction rates increase rates of mantle corner flow. Thus, the thermal gradients away from the cool slab into the hot mantle wedge interior are higher (spatially more confined to the slab) for faster subduction. Indeed, lava geochemistry indicates higher mantle temperature for the Lau and Manus back-arc basins that are behind faster subduction systems than for the more slowly subducting Scotia and Mariana systems [*Taylor and Martinez*, 2003].

3. LAU SPREADING CENTERS

The Lau Basin has multiple spreading systems, several of which remain incompletely mapped, indicated on the new compilation of multibeam data (Plate 1). The ELSC and CLSC, together with a short relay zone referred to as the Intermediate Lau spreading center (ILSC), were first mapped and identified in a Gloria sidescan sonar survey [*Parson et al.*, 1990]. That cruise identified southward propagation of the ELSC, which in turn is being replaced by southward propagation of the CLSC. To the north of 18°S, basin complexity increases. Northward, the CLSC merges with the Lau Extensional Transform Zone (LETZ), which in turn merges with the Peggy Ridge transform fault [*Zellmer and Taylor*, 2001]. To the east of the LETZ, the Fonualei Rift and spreading center (FRSC) [*Zellmer and Taylor*, 2001] is propagating southward into the volcanic front. This spreading center intersects the Mangatolu triple junction, which has a spreading axis extending northward to the trench [*Wright et al.*, 2000] and a short rift as its western arm [*Zellmer and Taylor*, 2001]. Various other spreading systems can be identified to the west, including the Futuna spreading system [*Pelletier et al.*, 2001], north of the Lau Ridge, and to the east of that the North-West Lau spreading center (NWLSC) [*Parson and Tiffin*, 1993; *Tiffin*, 1993] and offset to the northeast is the Niuafo'ou spreading center (NSC). Because of complicating factors—including effects of a slab tear at the northern end of the Tonga Trench [*Millen and Hamburger*, 1998], the likely influx of Samoan mantle plume material across this tear [*Turner and Hawkesworth*, 1998] possibly affecting melting characteristics, the existence of complex microplate tectonics partitioning extension across multiple spreading centers [*Pelletier et al.*, 1998], and large gaps in mapping between systems and consequently poorly known kinematic interactions—we focus below on the effects of arc proximity on the simpler and better known spreading centers south of 18°S.

3.1. Eastern Lau Spreading Center

The ELSC, ~400 km long, is the longest spreading ridge associated with the opening of the Lau basin behind the Tonga subduction zone (Plate 1) [*Parson et al.*, 1990; *Parson and Wright*, 1996; *Taylor et al.*, 1996]. The ELSC and Tofua AVF have linear geometries that progressively converge southward (from ~110 to within 40 km; see Plate 1). The ELSC thus transects obliquely across the part of the mantle wedge where geochemical gradients are pronounced [*Pearce et al.*, 1995; *Taylor and Martinez*, 2003] and result in distinct geophysical effects distributed over the 400-km length of the axis [*Martinez and Taylor*, 2002]. We refer here to the entire first-order spreading center between 19°20′S and 22°45′S as the ELSC (Plate 1). It can be subdivided at second-order (nontransform) offsets into three main subsegments having different axial morphologies: the shallow (1600–2000 m) and peaked VFR at the southern end from 22°45′S to 21°26′S (Plate 2); a deeper ridge (2000–2500 m) with a rounded axial high, the central ELSC (C-ELSC) from 21°26′S to 20°32′S (Plate 3); and an even deeper axis (2500–3000 m) with a nearly flat but faulted seafloor, the northern ELSC (N-ELSC) from 20°32′S to 19°20′S (Plate 4). Although the ELSC has no transform faults, second-order en-echelon and overlapping segments offset the axis by up to 5.5 km. The absence of large offsets thus minimizes segmentation effects [*Phipps Morgan and Forsyth*, 1988] on mantle upwelling, crustal accretion, and local thermal structure. As the ELSC approaches the AVF, spreading rates decrease from 96 to 39 mm/yr [*Zellmer and Taylor*, 2001]. Previous studies have shown that concentrations of water and slab-derived elements in ELSC-erupted lavas decrease northward, as does overall chemical depletion [*Ewart et al.*, 1994; *Pearce et al.*, 1995; *Taylor and Martinez*, 2003], the VFR showing a strong arc-like geochemical influence [*Jenner et al.*, 1987; *Frenzel et al.*, 1990; *Vallier et al.*, 1991]. Axial and near-axis depths (Plate 1) and mantle Bouguer anomalies [*Martinez and Taylor*, 2002] increase northward, indicating thinner crust. This interpretation is consistent with the two available seismic measurements of crustal thickness in the area of the axis of about 9 km at 22°10′S on the VFR [*Turner et al.*, 1999] and 5.5 km at extinct N-ELSC segments near 18°33′S [*Crawford et al.*, 2003]. Relative to a typical MOR crustal thickness of about 6 km over a broad range of spreading rates [*Chen*, 1992], the N-ELSC appears to have a deficient magmatic budget, whereas the budget of the VFR is excessive. This is consistent with other geophysical indicators of relative magmatic budget [*Scheirer and Macdonald*, 1993], which include the presence of an axial magma lens reflector beneath the VFR and C-ELSC but not beneath the N-ELSC [*Harding et al.*, 2000] and the northward decreasing axial cross-sectional area [*Martinez and Taylor*, 2002]. The evolution of these crustal properties can be traced in the ridge flanks as distinct terrains formed when the ELSC propagated southward [*Martinez and Taylor*, 2002]. The presence of these distinct terrains is consistent with systematic changes in magmatic production as the position of the spreading centers change relative to the AVF.

3.2. Valu Fa Ridge

The VFR comprises the southernmost well-organized segments of the ELSC seafloor spreading system. We group the morphologically distinctive segments with peaked axial highs between 22°45′S and 21°26′S as making up the VFR (Plate 2). Based on the Australia-Tonga Euler pole of *Zellmer and Taylor* [2001], the VFR opens at 39–61 mm/yr full rate and is

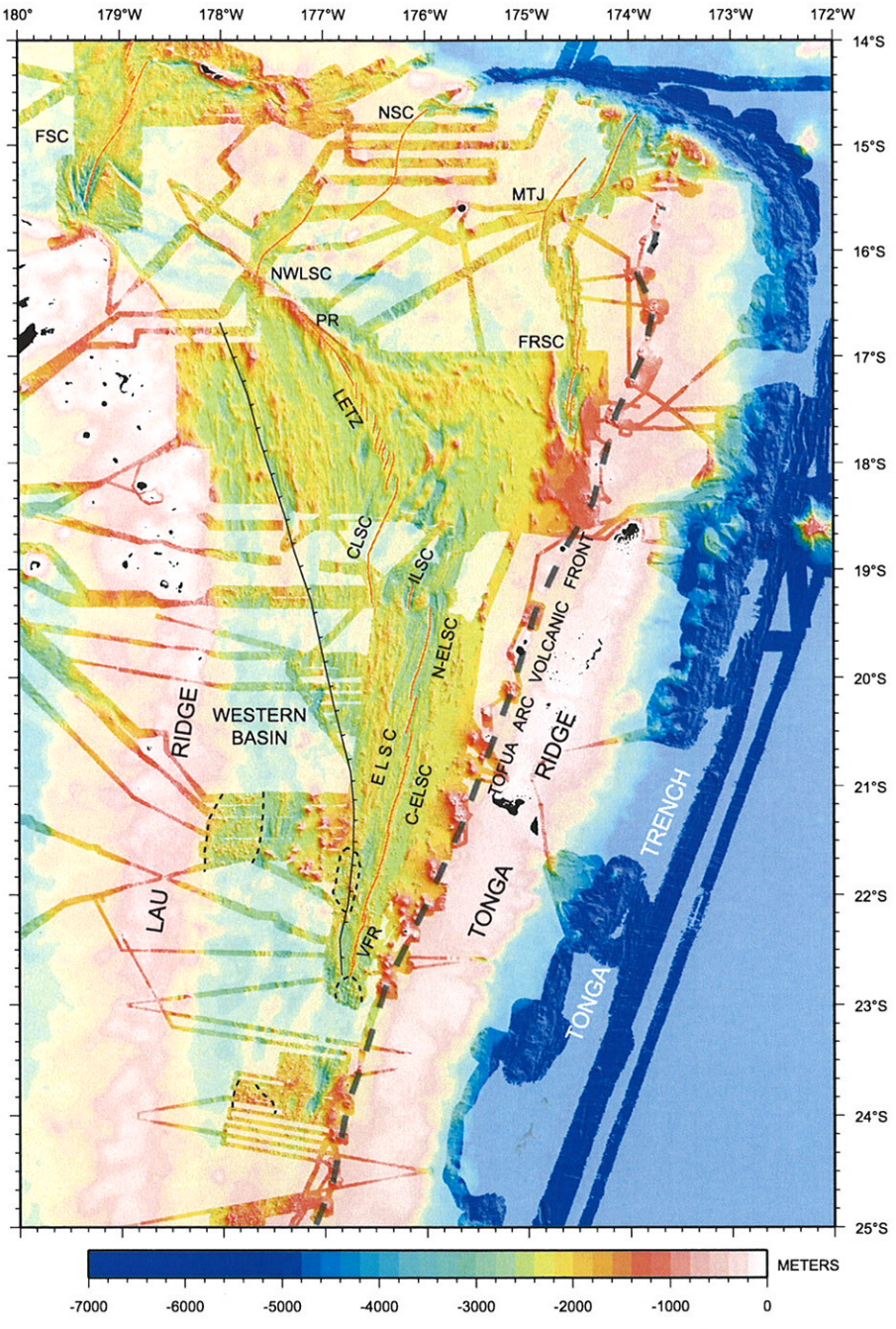

Plate 1. Compiled swath bathymetry data overlaid on regional background consisting of satellite-predicted bathymetry [*Smith and Sandwell*, 1997] and a previous compilation in the area north of 23°S [*Zellmer and Taylor*, 2001]. Identified spreading centers and other plate boundaries are shown with red lines: Eastern Lau spreading center (ELSC); Valu Fa Ridge (VFR); central Eastern Lau spreading center (C-ELSC); northern Eastern Lau spreading center (N-ELSC); Intermediate Lau Spreading Center (ILSC); Central Lau Spreading Center (CLSC); Lau Extensional Transform Zone (LETZ); Peggy Ridge (PR); North-West Lau spreading center (NWLSC); Futuna spreading center (FSC); Niuafo'ou spreading center (NSC); Mangatolu Triple Junction (MTJ); Fonualei Rift and spreading center (FRSC). Ticked line shows the western propagation boundary (pseudofault) of the ELSC (the eastern conjugate is presumably buried beneath the arc or arc volcaniclastic sediments and not identified). Thick dashed line shows the Tofua arc volcanic front (AVF). Thin dashed line delimits "ridges and knolls" terrain, here interpreted as distributed magmatic crustal accretion.

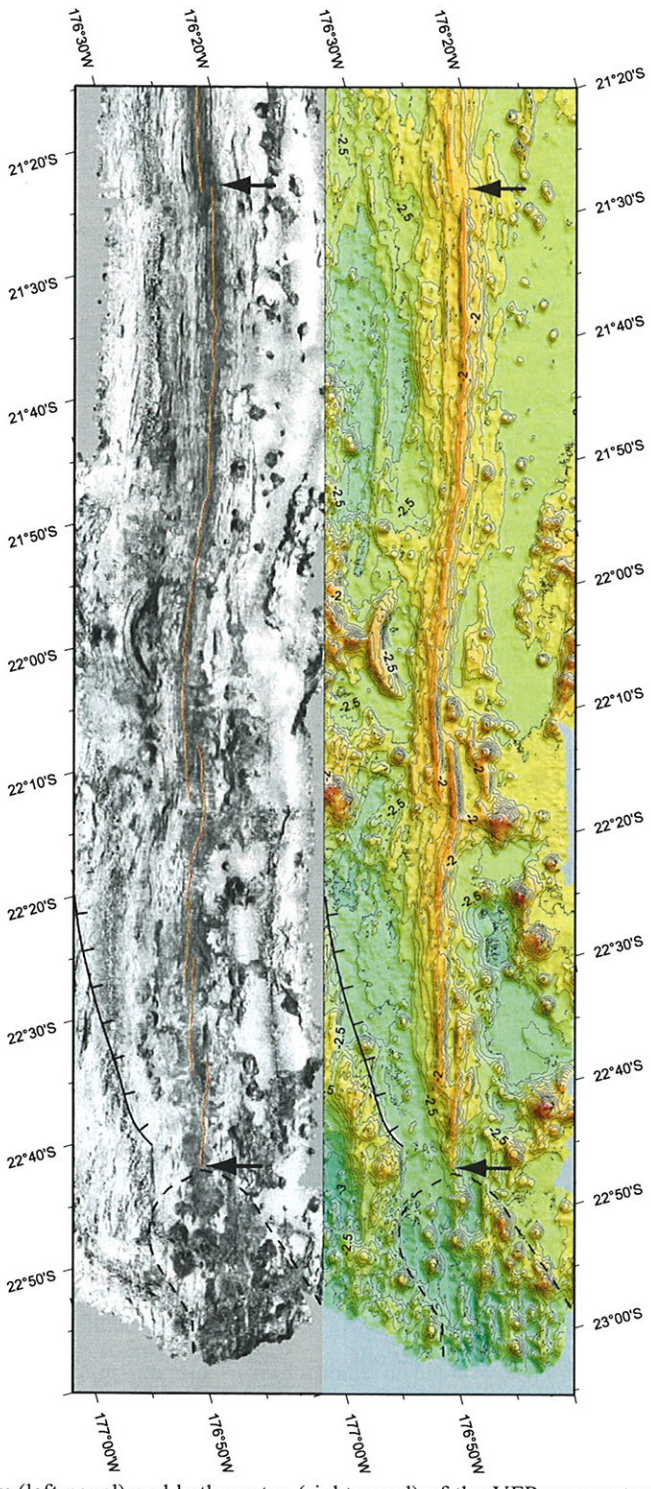

Plate 2. Acoustic imagery (left panel) and bathymetry (right panel) of the VFR segments shown delimited between arrows. Red line shows ridge axis and ticked line the ELSC pseudofault. Dashed line delimits the "ridges and knolls" terrain interpreted as a distributed zone of crustal accretion to the south of the VFR. Imagery is from a Simrad EM120 multibeam, where dark shades indicate high backscatter. Bathymetry map is contoured in 100-m intervals labeled in kilometers. See Plate 1 for color scale.

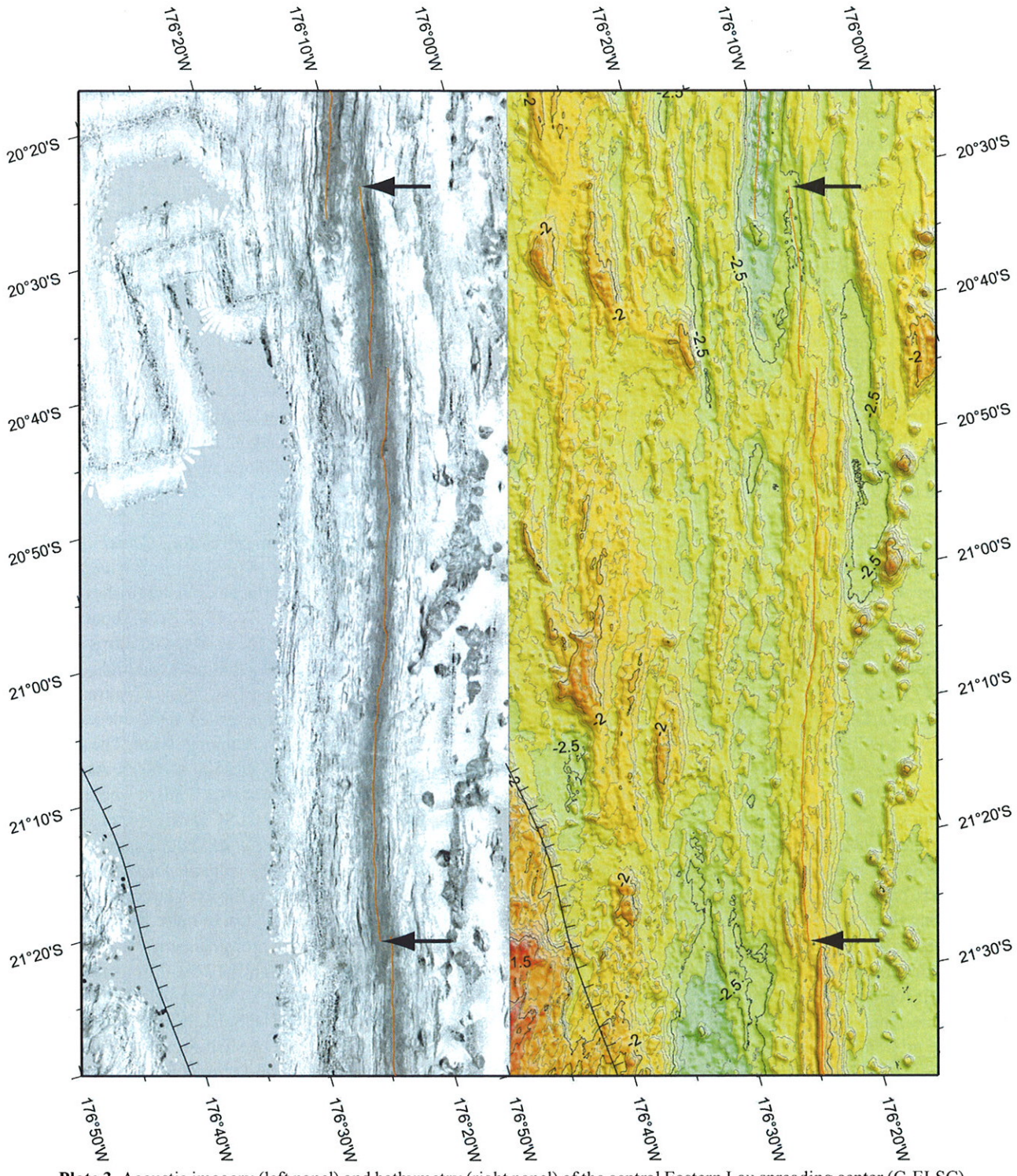

Plate 3. Acoustic imagery (left panel) and bathymetry (right panel) of the central Eastern Lau spreading center (C-ELSC) delimited between arrows. The ridge axis is shown as red line and the propagation boundary is shown as a ticked line. Imagery is from a Simrad EM120 multibeam, where dark shades indicate high backscatter. Bathymetry map is contoured in 100-m intervals labeled in kilometers. See Plate 1 for color scale.

located 40–60 km from the AVF (Plate 1). The southern end of the VFR is the limit of organized spreading and is propagating southward into a diffuse magmatic zone of opening (see below). Further south, between 23°30′S and 24°S, a deep graben has been mapped and interpreted as the southern limit of the ELSC and Lau Basin extension [*Fujiwara et al.*, 2001; *Ruellan et al.*, 2003]. The VFR has been the most studied part of the ESLC—first a result of Tripartite (United States, New Zealand, and Australian) mineral resource exploration in the area [*Scholl and Vallier*, 1985], the discovery of a magma chamber reflector beneath the ridge [*Morton and Sleep*, 1985], and subsequent discovery of hydrothermal "black smoker" vents [*Fouquet, et al.*, 1991]. The southernmost VFR consists of a series of short en-echelon and overlapping ridge segments at depths of 1600–2000 m [*Collier and Sinha*, 1990, 1992b; *Wiedicke and Collier*, 1993] that become one continuous segment by 22°10′S. Individual segments form narrow, steep-sided ridges with small summit volcanic cones [*Wiedicke and Collier*, 1993] (Plate 2), but in places there are broader axial swellings and the small volcanic cones often have summit pit craters visible in deep-towed sonar data [*Martinez et al.*, 2006]. Several of these axial swells have low backscatter and variegated textures, indicating volcaniclastic material draping the volcanic cones and ridge slopes, although darker lobate forms indicate that lava flows also occur (Plate 2). Most of the axial topographic relief, which can reach 100 m or more, appears to be volcanic, not tectonic, in nature [*Collier and Sinha*, 1992b; *Wiedicke and Collier*, 1993], consistent with the fact that the entire VFR is underlain by a nearly continuous but deep (up to 2200 ms two-way travel time) magma chamber reflector [*Morton and Sleep*, 1985; *Collier and Sinha*, 1990, 1992a; *Harding et al.*, 2000]. Overall, the VFR axis is shallowest near the overlapping spreading limbs between 22°10′S and 22°15′S, where axial relief is also largest, and where the axial magma chamber is broadest and continuous beneath both limbs and overlap basin [*Collier and Sinha*, 1992a]. Axial relief decreases markedly along the northern quarter of the VFR. Lineations, sometimes occurring in sets, are apparent in deep-towed and multibeam sidescan imagery and indicate small faults or fissures, but their topographic relief is minor (10s of m) relative to the volcanic features. The sidescan lineations, however, become more pronounced, longer, and more numerous northward along the VFR, although their relief remains smaller than that of the volcanic features. North of ~22°15′S, a few more prominent faults begin to develop.

3.3. Central Eastern Lau Spreading Center

The C-ELSC is about 90 km long and is offset from the VFR across a small (~2 km) nontransform discontinuity at 21°26′S (Plate 3). As with the VFR, C-ELSC segments are distinguished morphologically. The C-ELSC loses the peaked axial high character of the VFR, the axis instead forming an irregular rounded high within a broader low-relief valley (Plate 3). C-ELSC axial depths are 2000–2500 m, with the axis occupying a narrow high along the southern ~18 km and a narrow cleft along most of the rest of the ridge. The near-axis morphology is dominated by narrow linear ridges and valleys with relief of up to a few hundred meters and spaced at ~1–2 km. Volcanic cones are minor relative to smooth and hummocky lava flows and fields of pillow mounds imaged by deep-towed sonar data [*Martinez et al.*, 2006]. Near axis, within the ~1.8 km of deep-towed sonar swaths, fault lineations are more abundant and continuous than at the VFR, the larger faults developing further off-axis and being spaced at subkilometer intervals across axis [*Martinez et al.*, 2006]. Although no seismic determinations of crustal thickness on the C-ELSC are available, its shallower depths relative to normal MORs, the presence of an axial magma lens reflector [*Harding et al.*, 2000], and volcanic morphology suggest a somewhat enhanced magmatic budget.

3.4. Northern Eastern Lau Spreading Center

An abruptly deeper and flat floor distinguishes the N-ELSC from the C-ELSC (Plate 4). The N-ELSC is about 160 km long and opens at 76–96 mm/yr; the axial region forms a rough floor 2500–3000 m deep without a distinct axial high. The juncture between the C-ELSC and N-ELSC forms a nontransform offset with high-backscatter axes identified in the sidescan sonar data separated by ~5 km and overlapping ~9 km. The southern end of the N-ELSC is at depths of 2600–2700 m. At the northern segment end, depths plunge to over 3000 m where the N-ELSC overlaps with the ILSC and CLSC [*Parson et al.*, 1990]. Deep-towed sonar data [*Martinez et al.*, 2006] show that near-axis morphology is dominated by volcanic forms—lava flows and pillow mounds. Further from the axis, large asymmetric faults develop with spacing of 2–3 km or more, and throws increase to ~100–200 m, forming a prominent abyssal hill fabric (Plate 4). This is larger relief than the ~50–75-m median absolute deviation globally found at MORs spreading faster than about 70 mm/yr [*Small*, 1998]. The N-ELSC lies within a northward widening valley bordered by shallower crust (Plate 4), which we infer from gravity data [*Martinez and Taylor*, 2002] is thicker and formed during a more magmatically robust stage when the spreading axis was closer to the AVF (similar to that presently accreted at the C-ELSC and VFR).

3.5. Intermediate Lau Spreading Center

The ILSC has been described as a relay zone within the nontransform ~75-km offset that separates the Central and

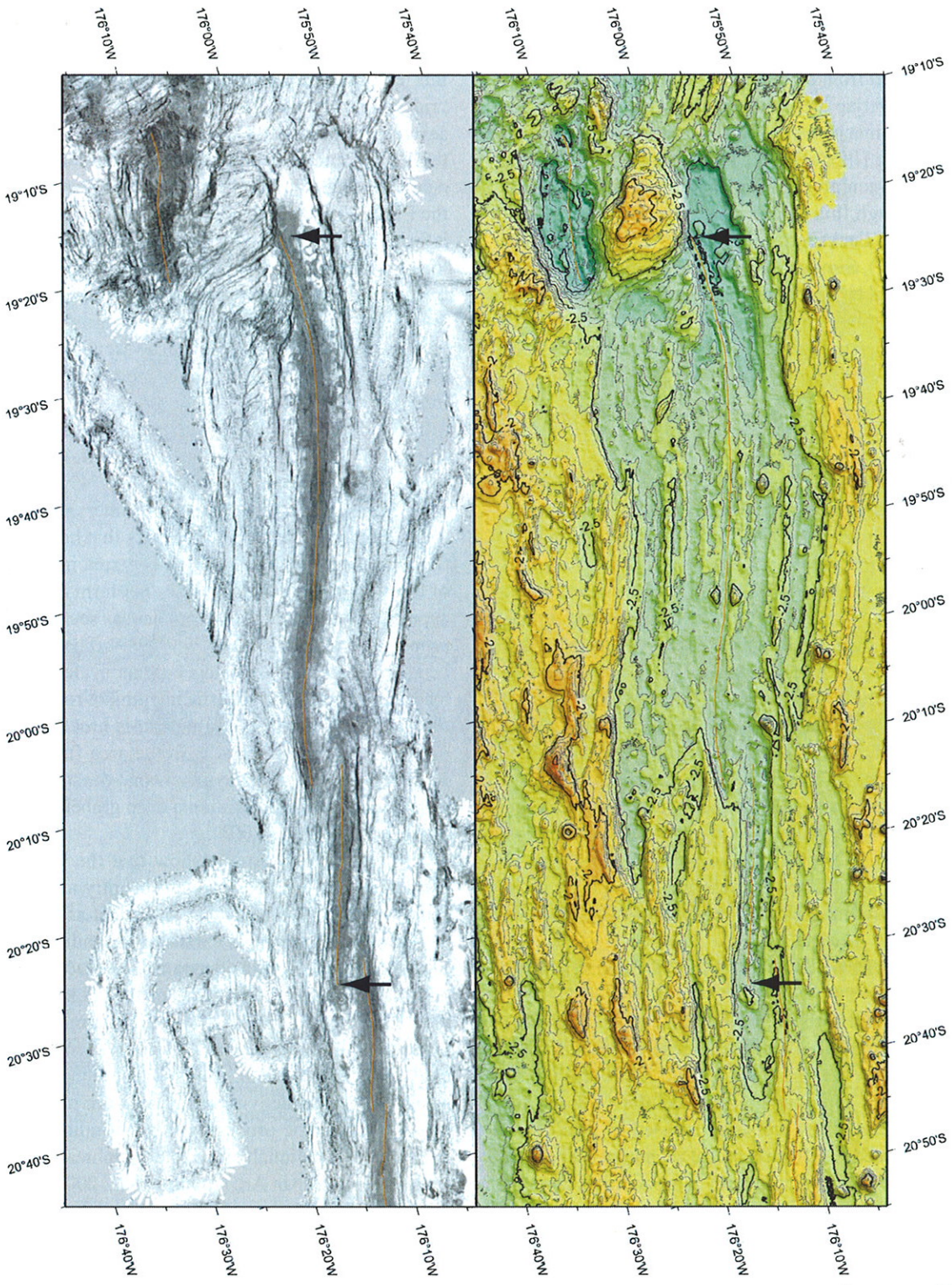

Plate 4. Acoustic imagery (left panel) and bathymetry (right panel) of the northern Eastern Lau spreading center (N-ELSC) delimited between arrows. The ridge axis is shown as red line. Imagery is from a Simrad EM120 multibeam, where dark shades indicate high backscatter. Bathymetry map is contoured in 100-m intervals labeled in kilometers. See Plate 1 for color scale.

Eastern Lau spreading centers [*Parson et al.*, 1990; *Wiedicke and Habler*, 1993] (Plate 5). Seafloor fabric in the vicinity of the ILSC is curved from azimuths of ~015° south of the axis to >070° in the overlap area between the ILSC and N-ELSC. Earthquake focal mechanisms are consistent with strike-slip bookshelf faulting [*Wetzel et al.*, 1993], as predicted for the overlap zone between propagating and failing ridges [*Hey et al.*, 1989]. Although this ridge segment is deep (~3200 m), its floor has high backscatter, indicating extensive recent volcanism (Plate 5). Similar shape and depth but sedimented features are located NNE of the ILSC. These have been interpreted as fossil grabens or spreading centers, formed like the ILSC in the overlap region between the CLSC and ELSC [*Parson et al.*, 1990; *Wiedicke and Habler*, 1993].

3.6. Central Lau Spreading Center

The CLSC extends from near 18°S to 19°20′S, where it ends in a narrow propagating ridge tip (Plate 5). To the north, the spreading center merges with the short left-stepping en-echelon ridge segments that make up the LETZ [*Zellmer and Taylor*, 2001]. The CLSC forms an axial high with summit depths of ~2250 m, except for the narrow propagating tip, which deepens to over 2400 m and forms a shallow valley [*Wiedicke and Habler*, 1993]. Along axis, away from the propagating tip, the CLSC morphology is like that of fast-spreading MORs—a broad axial high and low along-axis relief. This contrasts with the shallower, more peaked axial high of the VFR, which has higher relief along the summit because of the presence of many small volcanic cones [*Wiedicke and Habler*, 1993]. Rock sampling shows that the compositions on the CLSC are MORB-like [*Pearce, et al.*, 1995]. The crust of the CLSC contrasts with the shallower and hummocky crust of the N-ELSC flank into which it is propagating.

4. "DIFFUSE" PATCHES OF SEAFLOOR SPREADING?

At the southern end of the VFR, the peaked axial-high segments transition rapidly to a deeper and generally flatter area, forming a distinctive terrain of ridges and small seamounts (Plate 2). The ridges approximately parallel the VFR and are spaced 3–5 km apart. They are superimposed by small (1–2 km diameter), spaced (5–10 km) conical seamounts. The area south of the VFR is associated with a broadening zone of high backscatter—as wide as about 20 km at the limit of the sidescan coverage (Plate 2). By comparison, the high backscatter zone surrounding the N-ELSC imaged with the same hull-mounted Simrad EM120 sonar on the Kilo Moana (Plate 4) is only about 5 km wide, although it is located >90 km from the AVF and probably experiences less sedimentation from the active arc. The small seamounts in this high backscatter region, and a few extending beyond it, also have high backscatter. This seafloor fabric is not unique to this area. Similar fabric occurs further to the south in the Havre Trough (the "ridges and knolls" fabric of *Fujiwara et al.* [2001]) and in several of the mapped areas in the western basin and flanking the VFR (Plate 1). Similar seafloor fabric occurs at ~21°45′S near the pseudofault that marks the southward propagation of the ELSC. Although the pseudofault is incompletely mapped, it forms abrupt boundaries in places, but to the south from that location, the pseudofault area commonly forms a gradational transition from the western basin to the crust formed at the VFR. The seafloor fabric within this gradational transition zone is oblique to both the overall trend of the pseudofault and VFR at 21°45′S but becomes more aligned with the VFR trend to the south.

The Euler pole location describing Tonga Ridge–Australia separation (25°S,177.7°W [*Zellmer and Taylor*, 2001]), is located to the south of the VFR tip (~22°45′S). This, together with extensional earthquakes in this interval [*Fujiwara et al.*, 2001; *Ruellan et al.*, 2003], indicates that basin opening continues to the south of the VFR. The area immediately south of the VFR morphologic tip does not form a deep nor does it appear to be dominated by tectonism as seen in models of rift propagation [*Kleinrock and Hey*, 1989]. The absence of a graben, large seafloor deepening, or other evidence of large-scale tectonic thinning and acoustic imaging of recent volcanism in this area suggests that magmatism is broadly accommodating the extension. Similarly, in the area further south, near 23°50′S, multibeam surveys show that the site of active extension is more focused, forming a deep graben [*Fujiwara et al.*, 2001; *Ruellan, et al.*, 2003].

The above observations show that the focused seafloor spreading of the VFR changes abruptly at 22°45′S. To the south a more distributed form of crustal accretion must also be taking up comparable extension, as indicated by the lack of obvious tectonic subsidence or graben formation and the broad area of high backscatter of the ridges and knolls terrain. Further to the south, however, magmatic production is apparently lower, as a large tectonic graben forms [*Fujiwara et al.*, 2001; *Ruellan et al.*, 2003]. These along-strike variations in magmatic productivity of the back-arc may be modulated by AVF magmatic processes that, as indicated by the geologically, gravitationally, and tomographically observed "hot fingers" in the Japan Arc [*Tamura et al.*, 2002; *Hasegawa and Nakajima*, 2004], are spaced and oriented transversely to the arc and back-arc basin. The variations result in discrete zones with greater crustal thickening relative to intervening areas extending rearward from the AVF [*Tamura et al.*, 2002]. These arc-transverse melt and mantle convective flow anomalies are likely to be better developed and expressed here because of the arc-proximity of the zone of extension and the slow

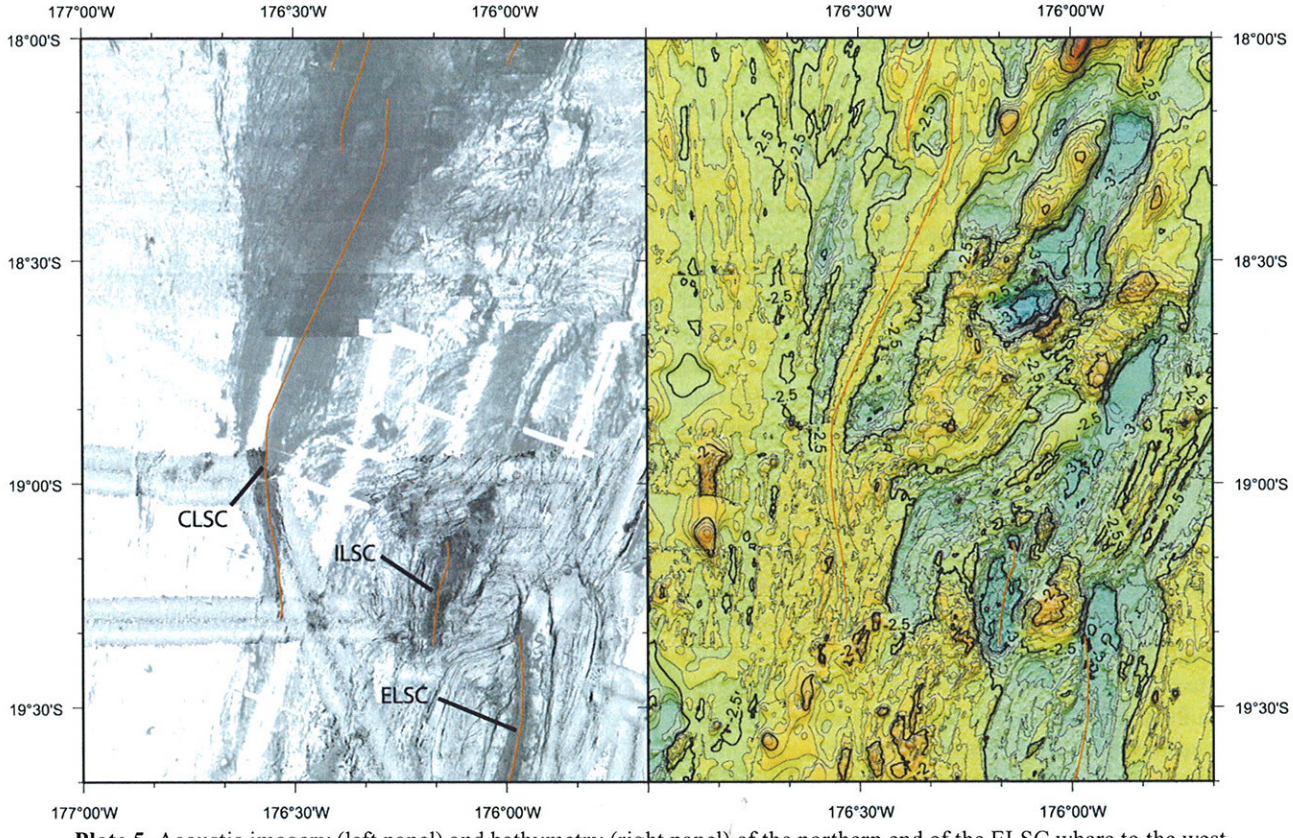

Plate 5. Acoustic imagery (left panel) and bathymetry (right panel) of the northern end of the ELSC where to the west it overlaps with the southward propagating CLSC and an extensional relay zone, the intermediate Lau spreading center (ILSC) [*Parson et al.*, 1990]. Imagery is a composite from HMR-1 north of ~18°40′S and Gloria data to the south overlaid with acoustic imagery from the hull-mounted Simrad EM120 multibeam system. Acoustic intensities have been qualitatively adjusted by eye to approximately the same values in overlap areas, the darker shades indicating higher backscatter values. Bathymetry map is contoured in 100-m intervals labeled in kilometers and includes digitized contours from *Zellmer and Taylor* [2001] in addition to multibeam data shown in Plate 1. See Plate 1 for bathymetry color scale.

opening rates in this part of the basin, which implies a smaller "plate-driven" spreading component of mantle advection and consequent magmatic production.

5. WESTERN LAU BASIN

Karig [1970] first interpreted the entire Lau Basin as formed by magmatic crustal accretion, although subsequent magnetic studies varied in the interpreted style and age of accretion [*Sclater et al.*, 1972; *Weissel*, 1977 *Malahoff et al.*, 1993]. Even after the propagating spreading development of the Lau basin was proposed based on Gloria sidescan imagery [*Parson et al.*, 1990], the whole basin was still inferred to have formed by seafloor spreading processes. Failed spreading centers in the western basin were identified [the "western Lau Spreading Center" of *Parson et al.*, 1990, their Figure 3] as well as localized areas of high backscatter interpreted as neovolcanic zones. Site survey data and other bathymetric compilations leading up to ODP Leg 135 in the Lau Basin [*Parson et al.*, 1992] began to change the interpretation of an entirely magmatic origin for the Lau Basin. The bathymetric compilations identified a western area interpreted to be dominated by horst and graben topography [*Parson et al.*, 1992]. Based on poorly correlated magnetic anomalies in the western basin and terrain characteristics inferred not to resemble MOR seafloor spreading fabric, the area west of the ELSC pseudofault was interpreted to be prespreading rifted terrain [*Parson and Hawkins*, 1994]. This terrain was thought to represent the tectonic disruption of the preexisting combined Lau/Tonga arc massif, the disruption being accompanied by rift-stage magmatic intrusion and extrusion. This rift evolution implied up to ~200 km of tectonic extension of preexisting arc basement in the southern Lau basin before organized seafloor spreading became established. The establishment of organized seafloor spreading was proposed to have propagated from near the Peggy Ridge southward and was inferred to largely terminate the rift phase of extension [*Parson and Hawkins*, 1994]. The area to the west of the pseudofault was termed the western extensional basin [*Hawkins*, 1995b] to distinguish it from crust formed by magmatic seafloor spreading.

At the time of the development of the "two-stage" model of Lau Basin development [*Parson and Hawkins*, 1994], the range of morphologic variability of the active magmatic spreading systems south of 18°S was not known. The primary synoptic mapping of large parts of those systems was derived from long-range GLORIA sidescan sonar imagery [*Parson et al.*, 1990], which can identify the neovolcanic zones but does not acquire bathymetric information. Bathymetric maps were largely compiled by interpolation across single-beam and narrow-swath (16 beams, swath width = ~73% of water depth [*de Moustier and Kleinrock*, 1986]) Sea Beam data [*Parson et al.*, 1992].

The new swath mapping data (Plates 6 and 7) indeed show a complex terrain in the western basin. The various landforms, however, have morphologic counterparts of equal or greater complexity and relief in the crust magmatically accreted at the active spreading centers to the east. We therefore critically reevaluate the two-stage rifting model and inferred nature of the western basin crust. We conclude that a magmatic origin for the entire Lau basin is a simpler explanation consistent with all of the data, as outlined below. Nevertheless, the terrains of the western basin remain incompletely mapped and show divergent trends from the evolution of the presently active magmatic systems south of 18°S. The western basin formed after the forearc breakup of the arc massif [*Hawkins and Allan*, 1994] during continued arc volcanism on the Lau Ridge [*Whelan et al.*, 1985] and before the complete readjustment of the arc magmatic systems that have been inferred to migrate across the evolving basin [*Clift and Dixon*, 1994; *Ewart et al.*, 1994; *Parson et al.*, 1994]. The terrains of the western basin may therefore reflect different magmatic processes from the purely "back-arc" active systems of the present day.

Following *Parsons and Hawkins* [1994], we refer herein to the terrain west of the ELSC propagation boundary and east of the Lau Ridge remnant arc as the "western basin" (Plate 1). Below we describe the terrain of the western basin from the various bathymetric surveys. Between ~16°50′S and 18°30′S the H-MR1 shallow-towed sonar (~100 m depth) has acquired nearly complete coverage sidescan imagery and bathymetry across the basin (Plate 6). The pseudofault identified as marking the ELSC southward propagation is shown in Plates 1 and 6. The western basin seafloor shows areas abyssal hill-like fabric comparable with that of ELSC spread crust to the east of the pseudofault, including a failed ridge propagation tip. The western basin fabric is less continuous, possibly as a result of greater ridge segmentation and propagation. A few areas form deeper and flatter sub-basins, most likely from sedimentation. Similar deeper, semienclosed areas flank the LETZ. The northwestern corner of the survey area and the region just to the west of the pseudofault have shallower and more volcanic terrain in places. The area to the west of the CLSC/LETZ high backscatter neovolcanic zones has generally lower backscatter than that to the east and becomes lower in intensity westward (Plate 6). Small localized areas of high backscatter occur to either side of the CLSC/LETZ. The largest of these in Plate 6 are associated with what appear to be volcanic highs near 17°S,177°40′W, 18°S,176°W, and 17°50′S,175°42′W, possibly indicating superimposed volcanoes.

Between ~21°10′S and 21°50′S, several multibeam bathymetry and sidescan imagery swaths map the area from the ELSC axis to near the Lau Ridge (Plate 7). The data show that the westernmost part of the basin is floored by a terrain resembling the "ridges and knolls" located to the south of the VFR

(Plate 2) and in several areas of the southernmost Lau Basin and Havre Trough [*Fujiwara et al.*, 2001]. The ridges and knolls fabric is delimited by a graben and a ridge to the east, which may represent the tip of an abandoned spreading center (Plate 7). These spatially associated terrains are similar to those in the present zone of active extension between 23°S and 24°S [*Fujiwara et al.*, 2001; *Ruellan et al.*, 2003], which include the southernmost VFR, the diffuse extension zone, and a graben to the south. The ridge and slightly overlapping small basin near 177°24′W is located near the area labeled as a fossil ridge in *Parson et al.* [1990] ("Western Lau Spreading Center", their Figure 3), and we infer that these structures represent part of a magmatic spreading system that became extinct when the ELSC propagated south. The area to the east of these structures and west of the pseudofault includes several volcanic centers. Their conical shapes indicate that they have not been extensively disrupted after formation although they are aligned over linear steps in the seafloor, which suggests that their emplacement may be fault controlled. All of the major conical volcanic features have low backscatter intensities, suggesting that they have not been recently active. These volcanic edifices may represent arc volcanism associated with the relocation of the AVF magmatism from the Lau Ridge to the present Tofua Arc after forearc rifting and breakup (see Figure 3). To our knowledge, these volcanoes have yet to be sampled, so their nature remains undetermined.

6. DISCUSSION

Our discussion of crustal accretion processes and their evolution in back-arc basins focuses on physical effects of the subduction setting and, in particular, on ways that such effects may result in the observed differences from MOR spreading. Our evaluation of possibly important processes is motivated by specific observations from back-arc basins, the Lau Basin in particular; however, gauging the degree of their interplay and relative importance is more difficult and will require integrated geophysical and geochemical studies between back-arc basins with different subduction parameters.

Back-arc basin development begins by rifting near the AVF so that the preexisting processes of arc magma generation and mantle wedge dynamics are important starting points in considering the subsequent evolution. Although a few models [*Conder et al.*, 2002] and observations [*Sisson and Bronto*, 1998] point to some role for decompression melting at volcanic fronts, most explain melt formation in the mantle wedge through fluxing mechanisms that lower the mantle solidus by the introduction of fluids released from the subducting slab [e.g., *Tatsumi and Eggins*, 1995]. Early models of arc melt formation and transport predicted simple periodic diapirs to result from these processes [*Marsh*, 1979]. Three-dimensional tomographic observations at the Japan Arc seismically image more complex mantle wedge processes. A low-velocity and high-attenuation sheet-like zone is located above and subparallel to the slab extending up-dip from about 150 km depth to the Moho, where it terminates beneath the AVF [*Hasegawa and Nakajima*, 2004]. This zone is interpreted as the location where fluids released from the slab have ascended into the hotter mantle wedge above and caused hydrous flux melting [*Hasegawa and Nakajima*, 2004]. The seismically identified sheet is locally thicker and displays lowest velocities in bands transverse to the AVF. In plan view the bands are spatially correlated with Bouguer gravity lows, indicating thickened crust, and the loci of arc and rear-arc volcanoes [*Tamura et al.*, 2002]. These associations have led to the interpretation that the arc-transverse bands are preferred arc melt transport channels or "hot fingers" [*Tamura et al.*, 2002]. Thus, infiltration of slab-derived fluids into the mantle wedge, mantle metasomatism, and melting may be spatially zoned within distinct sheets above the slab with focused bands transverse to the AVF and intervening areas much more like the ambient MORB-source. Such a spatial segregation of mantle wedge composition and processes that form arc melt may explain the discrete loci of arc volcanoes with much more MORB-like compositions in intervening rifts at the Izu-Bonin arc [*Fryer et al.*, 1990; *Hochstaedter et al.*, 1990a, 1990b]. Depending on the locus of arc rifting, these preexisting arc melt generation and transport processes may be variably disrupted as early MOR-type of advection develops and a back-arc basin forms.

By the time back-arc seafloor spreading is well-established in mature back-arc basins, mantle dynamics at the spreading centers are probably very much like those at MORs—primarily driven by surface plate separation that leads to mantle advection and pressure release melting [*Reid and Jackson*, 1981; *Phipps Morgan and Forsyth*, 1988]. During early basin evolution or when back-arc magmatic centers are near the AVF, interaction between the arc-transverse "hot fingers" and arc-parallel back-arc convective systems may be expected. Thus the AVF convective patterns oriented transversely to the arc may modulate back-arc rift advective patterns oriented mostly along-strike, as supported by along-strike geochemical variations in the southern Mariana Trough [*Gribble et al.*, 1996]. These arc/back-arc interactions may be more evident at slow extension rates when the back-arc plate-driven systems are weaker. At faster rates, greater mantle flux though seafloor spreading melting regimes may entrain large volumes of arc-source and ambient (MORB-source) mantle. The resulting crustal thickness will reflect the integrated sources but individual samples may still retain the distinct character of the various components [e.g., *Volpe et al.*, 1990].

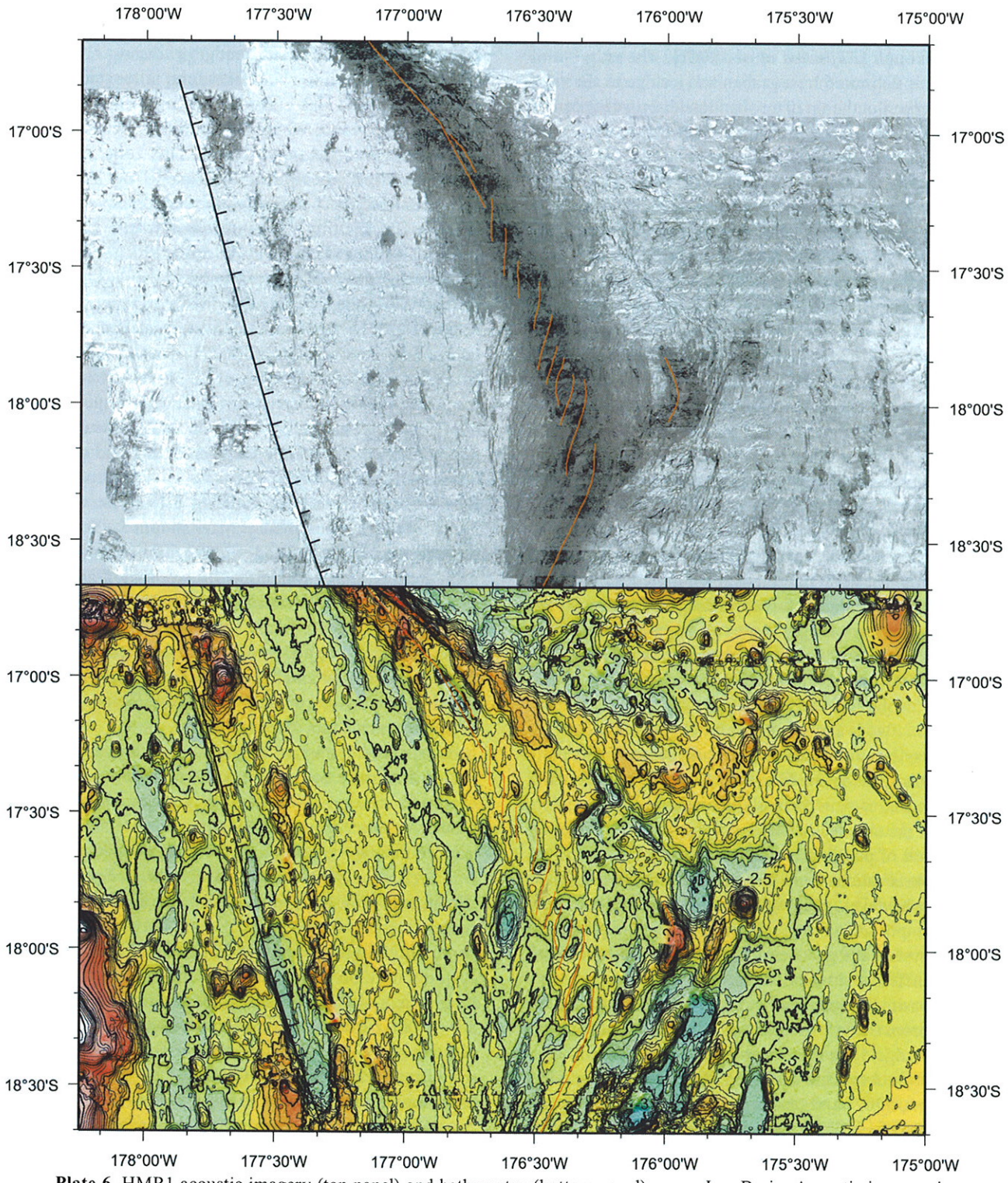

Plate 6. HMR1 acoustic imagery (top panel) and bathymetry (bottom panel) across Lau Basin. Acoustic imagery is shown with high backscatter indicated by dark shading. Bathymetry is contoured in 100-m intervals labeled in kilometers. See Plate 1 for bathymetry color scale. Ticked line indicate the location of the pseudofault formed by the southward propagation of the ELSC [*Parson et al.*, 1990], which delimits the western basin (to the west) from crust formed on the ELSC. Spreading segments and elements of the LETZ are shown with red lines.

Observations along arc-proximal spreading centers show varying magmatic productivity with separation from the AVF. Near the AVF, magma production rates are high, producing shallow thickened crust at the VFR [*Turner et al.*, 1999]. High water contents and strong arc geochemical characteristics in these lavas indicate that mantle chemistry is probably the primary cause of the increased melt productivity. Other possibilities include diversion of part of the arc magma budget to the spreading center itself [*Martinez et al.*, 2000] and changes in mantle flow dynamics. Modeling of mantle flow beneath MORs suggests that, at sufficiently low mantle viscosities, buoyancy forces can advect mantle beneath a ridge faster than predicted by purely plate-driven spreading [*Sotin and Parmentier*, 1989; *Su and Buck*, 1993], resulting in greater melt production. At arc-proximal back-arc ridges, low mantle viscosity may result from hydration by the subducting slab, thereby increasing melting by enhancing buoyancy-driven flow. However, increasing extents of melting proportional to water content is a consistent feature of back-arc lavas [*Stolper and Newman*, 1994; *Gribble et al.*, 1998; *Newman et al.*, 2000], suggesting a primary role of chemistry (water content) in enhancing melt productivity. Thus, both hydrous melting and mantle dynamics may be involved in the enhanced magmatic productivity of arc-proximal magmatic centers, but both mechanisms are ultimately related to water released from the slab. Farther from the AVF, thinner than normal crust is observed at the N-ELSC. In this area, occasional samples have highly depleted chemistries, but most do not [*Pearce et al.*, 1995]. Therefore the thinner than normal crustal thickness of the N-ELSC appears to reflect diminished melt delivery from mantle that is melting to nearly normal extents. We explain this by suggesting that corner flow recirculates refractory mantle (having had melt extracted at the arc or back-arc) downward and beneath the basin by viscous coupling with the slab. Water released from the slab may hydrate the refractory mantle, causing it to decrease in viscosity and form buoyant diapirs that rise into the mantle wedge. As these blobs of refractory mantle are entrained in the flow of seafloor spreading melting regimes, they displace more fertile (MORB-source) mantle, thereby lowering total melt production while the bulk of the lavas retain normal chemistry. Evidence for this mechanism may be found in the occasional highly depleted lavas sometimes sampled at the ELSC [*Pearce et al.*, 1995]. When spreading centers separate sufficiently from the AVF, they are largely removed from these subduction effects; they advect essentially MORB-source mantle and acquire MOR characteristics. This appears to be the case at the CLSC, located >170 km from the AVF. Lava chemistries there are predominantly MORB-like and the axial morphology is consistent with that of fast-spreading MORs.

This apparently systematic progression from "enhanced" to "deficient" to "normal" melt productivity with increasing separation from the AVF has also been noted in the active magmatic centers of the Mariana and Manus basins [*Martinez and Taylor*, 2003]. However, such a model predicts that the earliest spreading phases, when the nascent spreading center is closest to the AVF, should be the most magmatically productive and arc-influenced. This is not always observed. In the northwestern Lau Basin, the crust adjacent to the remnant Lau Ridge has linear seafloor spreading abyssal hills (although with apparent ridge propagation discontinuities) rather than the shallower, more chaotic and volcanic morphology of the VFR or parts of the ELSC flanks. Still other areas flanking the Lau Ridge appear even smoother (near 20°S) or covered by the "ridges and knolls"-type terrain (near 21°30′S). The large gaps in swath sonar coverage between these areas prevent a clear view of the spatial extents of these distinct terrains or of the transitions between them along strike. Because the Miocene Lau arc rifted in the forearc and Lau Ridge arc tholeiitic volcanism continued to 2.5 Ma, the evolution of the western Lau Basin differs significantly from the apparently more systematic development of the presently active back-arc magmatic systems. The history of migration of arc volcanism across the developing basin and the reestablishment of the AVF is poorly constrained. Additional controls on the interaction between back-arc and arc magmatic processes will probably be determined by mechanical and kinematic slab parameters such as dip, length, and subduction rate of the slab that affect mantle wedge convective patterns.

Although, as outlined above, the western basin has probably experienced a different tectonic evolution from that of the basin to the east, we consider that both were formed primarily by magmatic crustal accretion rather than by a two-stage evolution of rift phase followed by organized seafloor spreading [*Parson and Hawkins*, 1994]. The arguments for a two-stage process were based on two points: (1) apparent differences in the magnetic field of the western basin from the better correlated lineations in the basin to the east; (2) apparent inconsistencies of the morphology of the western basin with that of seafloor spreading at MORs [*Parson and Hawkins*, 1994]. A subsequent three-dimensional magnetization reduction (which reduces disturbances caused by predictable components of field skewness and topography) in fact shows magnetic lineations in the northern part of the western basin that correlate with lineated seafloor fabric [*Zellmer and Taylor*, 2001]. Large areas of the western basin south of the H-MR1 mapping (Plate 1) remain without full swath bathymetry and closely spaced magnetic measurements, limiting our ability to carry out similar analysis. The morphologic arguments for a two-stage Lau Basin evolution were based largely on the complexity and dissimilarity of the fabric of the western basin from MORs [*Parson et al.*, 1992]. As shown above, however, western basin fabrics have counterparts that formed by magmatic crustal accretion at the presently active Lau spreading centers, which themselves also depart from MOR characteristics.

Other arguments for a magmatic crustal accretion origin for the western Lau Basin include the lack of recovery of any

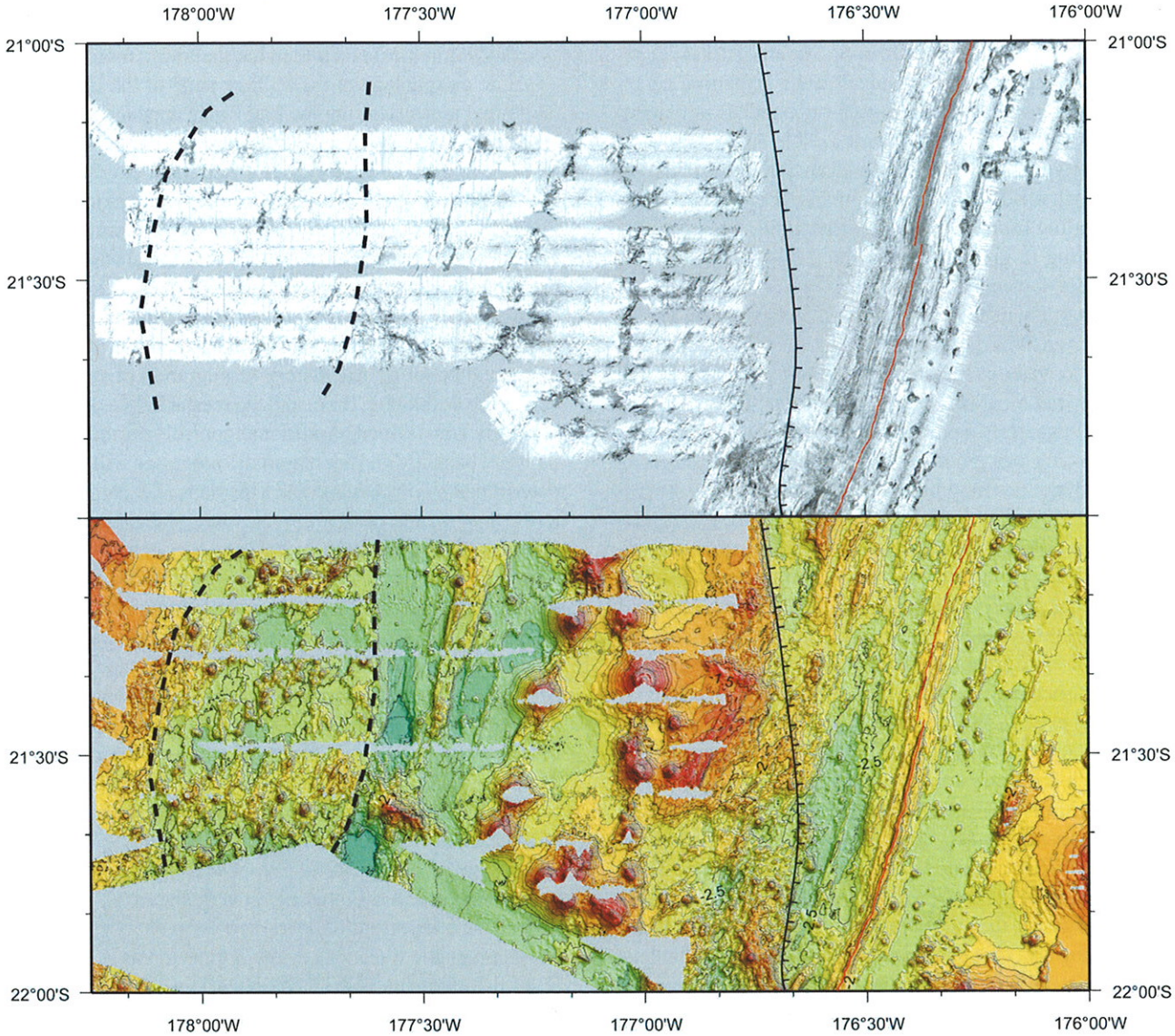

Plate 7. Acoustic imagery (top panel) and bathymetry swaths (bottom panel) crossing from the ELSC to the western basin. Acoustic imagery (Simrad EM120) is shown with high backscatter indicated by dark shading; bathymetry is contoured in 100-m intervals labeled in kilometers. See Plate 1 for bathymetry color scale. Spreading center is shown with red line. ELSC pseudofault is shown with ticked line. The dashed line delimits an interpreted fossil "ridges and knolls" terrain of distributed crustal accretion analogous to the active example interpreted to exist to the south of the Valu Fa Ridge (see Plate 2).

samples consistent with old rifted arc crust. The predecessor Lau/Tonga arc has an Eocene–Oligocene basement superposed by Miocene volcanics, which is exposed in areas of the Lau Ridge and Tonga forearc. No drilling samples (of basement beneath sedimented deeps) [*Hawkins et al.*, 1994] nor previous dredging of the high standing blocks [*Hawkins and Melchior*, 1985] have recovered samples with ages older than the opening age of the basin (~6 Ma). Drilling of the site closest to the Lau Ridge (ODP Site 834) recovered some of the most MORB-like samples [*Hawkins and Allan*, 1994].

The seismic structure of the western basin also is consistent with a magmatic origin. *Crawford et al.* [2003] analyzed a transect of ocean bottom seismometer (OBS) refraction data crossing from the Pacific plate to the Lau Ridge. In particular, their OBS transect crossed the pseudofault separating the western basin and the crust formed on the ELSC. Although they found large differences between the magmatically accreted crust of the ELSC and CLSC, there was no significant change in crustal thickness or velocity structure between the crust created in the western basin and that formed at the ELSC [*Crawford et al.*, 2003].

7. CONCLUSIONS

The generation of crust in back-arc basins is subject to multiple controls as a result of evolution above subduction zones. The position of the back-arc magmatic centers with respect to a variable rheology and fertility mantle wedge leads to large changes in melt productivity, composition, and mode of emplacement. The Lau Basin spreading centers south of 18°S exhibit apparently systematic trends along the spreading axes reflected in the flanking seafloor. Similar trends are also observed in the active spreading centers of other back-arc basins. The earliest formed western Lau Basin crust, which we infer is also magmatically created, does not follow similar patterns with arc proximity as occurs in the currently active spreading centers. We infer that the early basin evolution, involving forearc rifting and reestablishment of the magmatic arc, may have exerted controls on crustal accretion different from those of the present-day back-arc setting. Nevertheless, the overall Lau Basin characteristics are consistent with a magmatic origin. Unlike at MOR, however, as back-arc magmatic centers approach an established AVF, gradients in mantle wedge composition and rheology rather than spreading rate become a primary control on crustal accretion.

Acknowledgments. We thank the following investigators and institutions who contributed multibeam bathymetry data to the compilation presented here: Richard Arculus, Jim Childress, Chuck Fisher, Toshiya Fujiwara, Charles Langmuir, Bernard Pelletier, Meg Tivey, Robert Vrijenhoek, Tim Worthington, the Korean Ocean Research and Development Institute (KORDI), and the Scripps Institute of Oceanography multibeam data base. We also thank Roy Livermore and Robert Stern for reviews. This work was supported by the US Ridge 2000 program (OCE-0242077). SOEST contribution number 6794.

REFERENCES

Bednarz, U., and H.-U. Schmincke (1994), Composition and origin of volcaniclastic sediments in the Lau Basin (Southwest Pacific), Leg 135 (Sites 834–839), in *Proceedings of the Ocean Drilling Program, Scientific Results*, edited by J. W. Hawkins, et al., pp. 51–74, Ocean Drilling Program, College Station, TX.

Billen, M. I., and M. Gurnis (2001), A low viscosity wedge in subduction zones, *Earth Planet. Sci. Lett.*, *193*, 227–236.

Billen, M. I., M. Gurnis, and M. Simons (2003), Multiscale dynamics of the Tonga-Kermadec subduction zone, *Geophys J Int*, *153*, 359–388.

Bloomer, S. H., R. J. Stern, and N. C. Smoot (1989), Physical volcanology of the submarine Mariana and Volcano Arcs, *Bull. Volcanol.*, *51*, 210–224.

Chen, Y. J. (1992), Oceanic crustal thickness versus spreading rate, *Geophys. Res. Lett.*, *19*, 753–756.

Chiu, J.-M., B. L. Isacks, and R. K. Cardwell (1991), 3-D configuration of subducted lithosphere in the western Pacific, *Geophys. J. Int.*, *106*, 99–111.

Clift, P. D., and J. E. Dixon (1994), Variations in arc volcanism and sedimentation related to rifitng of the Lau Basin (Southwest Pacific), in *Proceedings of the Ocean Drilling Program, Scientific Results*, edited by J. W. Hawkins, et al., pp. 23–45, Ocean Drilling Program, College Station, TX.

Collier, J., and M. Sinha (1990), Seismic images of a magma chamber beneath the Lau Basin back-arc spreading centre, *Nature*, *346*, 646–648.

Collier, J. S., and M. C. Sinha (1992a), Seismic mapping of a magma chamber beneath the Valu Fa Ridge, Lau Basin, *J. Geophys. Res*, *97*, 14031–14053.

Collier, J. S., and M. C. Sinha (1992b), The Valu Fa Ridge: The pattern of volcanic activity at a back arc spreading centre, *Marine Geol.*, *104*, 243–263.

Conder, J. A., D. A. Wiens, and J. Morris (2002), On the decompression melting structure at volcanic arcs and back-arc spreading centers, *Geophys. Res. Lett.*, *29*, 20, 21–24, DOI: 10.1029/2002GL015390.

Crawford, W. C., J. A. Hildebrand, L. M. Dorman, S. C. Webb, and D. A. Wiens (2003), Tonga Ridge and Lau Basin crustal structure from seismic refraction data, *J. Geophys. Res*, *108*, doi:10.1029/2001JB001435.

Davies, J. H., and D. J. Stevenson (1992), Physical model of source region of subduction zone volcanics, *J. Geophys. Res*, *97*, 2037–2070.

de Moustier, C., and M. C. Kleinrock (1986), Bathymetric artifacts in Sea Beam data: how to recognize them and what causes them, *J. Geophys. Res*, *91*, 3407–3424.

Deschamps, A., and T. Fujiwara (2003), Asymmetric accretion along the slow-spreading Mariana Ridge, *Geochem., Geophys., Geosyst.*, *4*, doi:10.1029/2003GC000537.

Dixon, T. H., and R.. Stern (1983), Petrology, chemistry, and isotopic composition of submarine volcanoes in the southern Mariana arc, *Geological Society of America Bulletin*, *94*, 1159–1172.

Evans, R. L., G. Hirth, K. Baba, D. Forsyth, A. Chave, and R. Mackie (2005), Geophysical evidence from the MELT area for compositional controls on oceanic plates, *Nature*, *437*, 249–252.

Ewart, A., W. B. Bryan, B. W. Chappell, and R. L. Rudnick (1994), Regional geochemistry of the Lau-Tonga arc and back-arc systems, in *Proceedings of the Ocean Drilling Program Leg 135, Scientific Results*, edited by J. Hawkins, et al., pp. 385–426, Ocean Drilling Program, College Station, TX.

Ewart, A., and C J. Hawkesworth (1987), The Pleistocene-Recent Tonga-Kermadec arc lavas: Interpretation of new isotopic and rare earth data in terms of a depleted mantle source model, *J. Petrol.*, *28*, 495–530.

Fouquet, Y., U. Von Stackelberg, J. L. Charlou, J. P. Donval, J. Erzinger, J. P. Foucher, P. Herzig, R. Muhe, S. Soakai, M. Wiedicke, and H. White-

church (1991), Hydrothermal activity and metallogenesis in the Lau back-arc basin, *Nature*, *349*, 778–781.

Frenzel, G., R. Muhe, and P. Stoffers (1990), Petrology of the volcanic rocks from the Lau Basin, southwest Pacific, *Geol. Jahrb.*, *92*, 395–479.

Fryer, P., H. Fujimoto, M. Sekine, L. E. Johnson, J. Kasahara, H. Masuda, T. Gamo, T. Ishii, M. Ariyoshi, and K. Fujioka (1998), Volcanoes of the southwestern extension of the active Mariana island arc: New swath-mapping and geochemical studies, *The Island Arc*, *7*, 596–607.

Fryer, P., B. Taylor, C. H. Langmuir, and A. G. Hochstaedter (1990), Petrology and geochemistry of lavas from the Sumisu and Torishima backarc rifts, *Earth Planet. Sci. Lett.*, *100*, 161–178.

Fujiwara, T., T. Yamazaki, and M. Joshima (2001), Bathymetry and magnetic anomalies in the Havre Trough and southern Lau Basin: from rifting to spreading in back-arc basins, *Earth Planet. Sci. Lett.*, *185*, 253–264.

Gaherty, J. B., T. H. Jordan, and L. S. Gee (1996), Seismic structure of the upper mantle in a central Pacific corridor, *J. Geophys. Res*, *101*, 22,291–222,309.

Garcia, M. O., N. W. K. Liu, and D. Muenow (1979), Volatiles in submarine volcanic rocks from the Mariana Island arc and trough, *Geochim. Cosmochim. Acta*, *43*, 305–312.

Govers, R., and M. J. R. Wortel (2005), Lithosphere tearing at STEP faults: Response to edges of subduction zones, *Earth Planet. Sci. Lett.*, *236*, 505–523.

Gribble, R. F., R. J. Stern, S. H. Bloomer, D. Stuben, T. O'hearn, and S. Newman (1996), MORB mantle and subduction components interact to generate basalts in the southern Mariana Trough back-arc basin, *Geochim. Cosmochim. Acta*, *60*, 2153–2166.

Gribble, R. F., R. J. Stern, S. Newman, S. H. Bloomer, and T. O'hearn (1998), Chemical and isotopic composition of lavas from the northern Mariana Trough: implications for magmagenesis in back-arc basins, *J. Petrol.*, *39*, 125–154.

Gudmundsson, O., and M. Sambridge (1998), A regionalized upper mantle (RUM) seismic model, *J. Geophys. Res*, *103*, 7121–7136.

Harding, A. J., G. M. Kent, and J. A. Collins (2000), Initial results from a multichannel seismic survey of the Lau back-arc basin, *Eos, Trans. AGU*, *81*, abstract T61C-16.

Hasegawa, A., and J. Nakajima (2004), Geophysical constraints on slab subduction and arc magmatism, in *The State of the Planet: Frontiers and Challenges in Geophysics, Geophys. Monogr. Ser.*, edited by R. S. J. Sparks and C. J. Hawkesworth, pp. pp. 81–94, American Geophysical Union, Washington, D.C.

Hawkins, J., L. Parson, and J. Allen (1994), *Proceedings Ocean Drilling Program, Scientific Results, Leg 135*, 984 pp., Ocean Drilling Program, College Station, TX.

Hawkins, J. W. (1994), Petrologic Synthesis: Lau Basin Transect (Leg 135), in *Proceedings of the Ocean Drilling Program Leg 135, Scientific Results*, edited by J. Hawkins, et al., pp. 879–905, Ocean Drilling Program, College Station, TX.

Hawkins, J. W. (1995a), Evolution of the Lau Basin—Insights from ODP Leg 135, in *Active Margins and Marginal Basins of the Western Pacific*, edited by B. Taylor and J. Natland, pp. 125–173, American Geophysical Union, Washington, D.C.

Hawkins, J. W. (1995b), The Geology of the Lau Basin, in *Backarc Basins: Tectonics and Magmatism*, edited by B. Taylor, pp. 63–138, Plenum Press, New York.

Hawkins, J. W., and J. F. Allan (1994), Petrologic evolution of the Lau Basin, sites 834–839, in *Proceedings of the Ocean Drilling Program Leg 135, Scientific Results*, edited by J. Hawkins, et al., pp. 427–470, Ocean Drilling Program, College Station, TX.

Hawkins, J. W., and J. T. Melchior (1985), Petrology of Mariana Trough and Lau Basin basalts, *J. Geophys. Res*, *90*, 11,431–411,468.

Hey, R. N., J. M. Sinton, and F. K. Duennebier (1989), Propagating rifts and spreading centers, in *The Eastern Pacific Ocean and Hawaii, The Geology of North America*, edited by E. L. Winterer, D. M. Hussong, R. W. Decker, pp. 161–176, Geological Society of America, Boulder, CO.

Hirth, G., and D. L. Kohlstedt (1996), Water in the oceanic upper mantle: implications for rheology, melt extraction and the evolution of the lithosphere, *Earth Planet. Sci. Lett.*, *144*, 93–108.

Hochstaedter, A. G., J. Gill, R. Peters, P. Broughton, P. Holden, and B. Taylor (2001), Across-arc geochemical trends in the Izu-Bonin arc: Contributions from the subducting slab, *Geochem. Geophys. Geosys.*, *2*, 2000GC000105.

Hochstaedter, AG., J. B. Gill, M. Kusakabe, S. Newman, M. Pringle, B. Taylor, and P. Fryer (1990a), Volcanism in the Sumisu Rift, I. Major element, volatile, and stable isotope geochemistry, *Earth Planet. Sci. Lett.*, *100*, 179–194.

Hochstaedter, A. G., J. B. Gill, and J. D. Morris (1990b), Volcanism in the Sumisu Rift, II. Subduction and non-subduction related components, *Earth Planet. Sci. Lett.*, *100*, 195–209.

Hochstaedter, A. G., J. B. Gill, B. Taylor, O. Ishizuka, M. Yuasa, and S. Morita (2000), Across-arc geochemical trends in the Izu-Bonin arc: Constraints on source composition and mantle melting, *J. Geophys. Res*, *105*, 495–512.

Honda, S., and T. Yoshida (2005), Application of the model of small-scale convection under the island arc to the NE Honshu subduction zone, *Geochem. Geophys. Geosyst.*, *6*, doi:10.1029/2004GC000785.

Hussong, D. M., and S. Uyeda (1981), Tectonic processes and the history of the Mariana arc: A synthesis of the results of Deep Sea Drilling Project Leg 60, in *Init. Repts. Deep Sea Drill. Proj.*, edited by D. M. Hussong and S. Uyeda, pp. 909–929, U. S. Government Printing Office, Washington D. C.

Jenner, G. A., P. A. Cawood, M. Rautenschlein, and W. M. White (1987), Composition of back-arc basin volcanics, Valu Fa ridge, Lau Basin: Evidence for a slab-derived component in their mantle source, *J. Volcanol. Geotherm. Res.*, *32*, 209–222.

Karato, S., and H. Jung (1998), Water, partial melting and the origin of the seismic low velocity and high attenuation zone in the upper mantle, *Earth Planet. Sci. Lett.*, *157*, 193–207.

Karig, D. E. (1970), Ridges and basins of the Tonga-Kermadec island arc system, *J. Geophys. Res*, *75*, 239–254.

Kleinrock, M. C., and R. N. Hey (1989), Detailed tectonics near the tip of the Galapagos 95.5°W propagator: how the lithosphere tears and a spreading axis develops., *J. Geophys. Res*, *94*, 13801–13838.

Kobayashi, K., S. Kasuga, and K. Okino (1995), Shikoku Basin and its margins, in *Backarc Basins: Tectonics and Magmatism*, edited by B. Taylor, pp. 381–405, Plenum Press, New York.

Kong, L. S., N. Seama, H. Fujimoto, J. Kasahara, and KH92-1 Shipboard Scientific Party (1992), Segmentation of the Mariana Trough Back-Arc Spreading Center at 18°N, in *InterRidge News*, *1*, 2–5.

Kong, L. S. L. (1993), Seafloor Spreading in the Mariana Trough, in *Preliminary report of the Hakuho-Maro Cruise KH92-1*, edited by J. Segawa, pp. 5–16, Ocean Research Institute, Tokyo.

Kusznir, N. J., and R. G. Park (1987), The extensional strength of the continental lithosphere: its dependence on geothermal gradient, and crustal composition and thickness, in *Continental Extensional Tectonics*, edited by M. P. Coward, et al., pp. 35–52, Geological Society of America.

Lagabrielle, Y., J. Goslin, H. Martin, J.-L. Thirot, and J.-M. Auzende (1997), Multiple active spreading centres in the hot North Fiji Basin (Southwest Pacific): a possible model for Archaean seafloor dynamics? *Earth Planet. Sci. Lett.*, *149*, 1–13.

Livermore, R., A. Cunningham, L. Vanneste, and R. Larter (1997), Subduction influence on magma supply at the East Scotia Ridge, *Earth Planet. Sci. Lett.*, *150*, 261–275.

Macdonald, K. C. (1982), Mid-ocean ridges: Fine scale tectonic, volcanic and hydrothermal processes within the plate boundary zone, *Annual Review of Earth and Planetary Science*, *10*, 155–190.

Maillet, P., E. Ruellan, M. Gerard, A. Person, H. Bellon, J. Cotten, J.-L. Joron, S. Nakada, and R. C. Price (1995), Tectonics, Magmatism, and Evolution of the New Hebrides Backarc Troughs (Southwest Pacific), in *Backarc Basins: Tectonics and Magmatism*, edited by B. Taylor, pp. 177–235, Plenum Press, New York.

Malahoff, A., L. W. Kroenke, N. Cherkis, and J. Brozena (1993), Magmetic and tectonic fabric of the north Fiji Basin and Lau Basin, in *Basin Formation, Ridge Crest Processes and Metallogenesis in the North Fiji Basin*, edited by L. W. Kroenke and J. V. Eade, pp. 49–61, Springer-Verlag, New York.

Marsh, B. D. (1979), Island arc development: some observations, experiments, and speculations, *J. Geol., 87*, 687–714.

Martinez, F., P. Fryer, N. A. Baker, and T. Yamazaki (1995), Evolution of backarc rifting: Mariana Trough, 20°–24°N, *J. Geophys. Res, 100*, 3807–3827.

Martinez, F., P. Fryer, and N. Becker (2000), Geophysical Characteristics of the Southern Mariana Trough, 11°50'N–13°40'N, *J. Geophys. Res, 105*, 16591–16607.

Martinez, F., and B. Taylor (2002), Mantle wedge control on back-arc crustal accretion, *Nature, 416*, 417–420.

Martinez, F., and B. Taylor (2003), Controls on back-arc crustal accretion: insights from the Lau, Manus and Mariana basins, in *Intra-oceanic subduction systems: tectonic and magmatic processes*, edited by R. D. Larter and P. T. Leat, pp. 19–54, Geological Society, London.

Martinez, F., B. Taylor, E. T. Baker, J. A. Resing, and S. L. Walker (2006), Opposing trends in crustal thickness and spreading rate along the back-arc Eastern Lau Spreading Center: Implications for controls on ridge morphology, faulting, and hydrothermal activity, *Earth Planet. Sci. Lett., 245*, 655–672.

McCulloch, M. T., and J. A. Gamble (1991), Geochemical and geodynamical constraints on subduction zone magmatism, *Earth Planet. Sci. Lett., 102*, 358–374.

MELT Seismic Team (1998), Imaging the deep seismic structure beneath a mid-ocean ridge: The MELT Experiment, *Science, 280*, 1215–1218.

Millen, D. W., and M. W. Hamburger (1998), Seismological evidence for tearing of the Pacific plate at the northern termination of the Tonga subduction zone, *Geology, 26*, 659–662.

Molnar, P., and T. Atwater (1978), Interarc spreading and Cordilleran tectonics as alternates related to the age of subducted oceanic lithosphere, *Earth Planet. Sci. Lett., 41*, 330–340.

Morton, J. L., and N. H. Sleep (1985), Seismic Reflections from a Lau Basin Magma Chamber, in *Geology and offshore resources of Pacific island arcs—Tonga region, Circum Pacific Council for Energy and Mineral Resources Earth Science Series*, edited by D. W. Scholl and T. L. Vallier, pp. 441–453, Circum Pacific Council for Energy and Mineral Resources, Houston, TX.

Muenow, D. W., M. R. Perfit, and K. E. Aggrey (1991), Abundances of volatiles and genetic relationships among submarine basalts from the Woodlark Basin, Southwest Pacific, *Geochim. Cosmochim. Acta, 55*, 2231–2239.

Newman, S., E. Stolper, and R. J. Stern (2000), H_2O and CO_2 in magmas from the Mariana arc and back arc systems, *Geochem. Geophys. Geosyst., 1*, 1999GC000027.

Nishizawa, A., K. Kaneda, Y. Katagiri, and J. Kasahara (2005), Crustal structure of the southern Kyushu-Palau Ridge, the other half of the proto Izu-Bonin-Mariana island arc, *Eos, Trans. AGU, 86*, abstract T53A-1409.

Okino, K., S. Kasuga, and Y. Ohara (1998), A new scenario of the Parece Vela Basin genesis, *Mar. Geophys. Res., 20*, 21–40.

Parson, L. M., and J. W. Hawkins (1994), Two-stage ridge propagation and the geological history of the Lau backarc basin, in *Proceedings of the Ocean Drilling Program, Scientific Results*, edited by J. W. Hawkins, et al., pp. 819–828.

Parson, L. M., J. W. Hawkins, and P. M. Hunter (1992), Morphotectonics of the Lau Basin seafloor-implications for the opening history of back-arc basins, in *Proceedings of the Ocean Drilling Program, Initial Reports*, edited by L. M. Parson, et al., pp. 81–82, Ocean Drilling Program, College Station, TX.

Parson, L. M., J. A. Pearce, B. J. Murton, R. A. Hodkinson, and RRS *Charles Darwin* Scientific Party (1990), Role of ridge jumps and ridge propagation in the tectonic evolution of the Lau back-arc basin, southwest Pacific, *Geology, 18*, 470–473.

Parson, L. M., R. G. Rothwell, and C. J. MacLeod (1994), Tectonics and sedimentation in the Lau Basin (Southwest Pacific), in *Proceedings of the Ocean Drilling Program, Scientific Results*, edited by J. W. Hawkins, et al., pp. 9–21, Ocean Drilling Program, College Station, TX.

Parson, L. M., and D. L. Tiffin (1993), Northern Lau Basin: Backarc extension at the leading edge of the Indo-Australian Plate, *Geo-Mar. Lett., 13*, 107–115.

Parson, L. M., and I. C. Wright (1996), The Lau-Havre-Taupo back-arc basin: A southward-propagating, multi-stage evolution from rifting to spreading, *Tectonophysics, 263*, 1–22.

Parsons, B., and J. G. Sclater (1977), An analysis of the variation of ocean floor bathymetry and heat flow with age, *J. Geophys. Res, 82*, 803–827.

Peacock, S. M. (1996), Thermal and petrological structure of subduction zones, in *Subduction: Top to Bottom*, edited by G. E. Bebout, D. W. Scholl, S. H. Kirby, and J. P. Platt, pp. 119–133, American Geophysical Union, Washington D. C.

Pearce, J. A., M. Ernewein, S. H. Bloomer, L. M. Parson, B. J. Murton, and L. E. Johnson (1995), Geochemistry of Lau Basin volcanic rocks: influence of ridge segmentation and arc proximity, in *Volcanism Associated with Extension at Consuming Plate Margins*, edited by J. L. Smellie, pp. 53–75, Geological Society, London.

Pelletier, B., S. Calmant, and R. Pillet (1998), Current tectonics of the Tonga-New Hebrides region, *Earth Planet. Sci. Lett., 164*, 263–276.

Pelletier, B., Y. Lagabrielle, M. Benoit, G. Cabioch, S. Calmant, E. Garel, and C. Guivel (2001), Newly identified segments of the Pacific-Australia plate boundary along the North Fiji transform zone, *Earth Planet. Sci. Lett., 193*, 347–358.

Phipps Morgan, J. (1997), The generation of a compositional lithosphere by mid-ocean ridge melting and its effect on subsequent off-axis hotspot upwelling and melting, *Earth Planet. Sci. Lett., 146*, 213–232.

Phipps Morgan, J., and D. W. Forsyth (1988), Three-dimensional flow and temperature perturbations due to a transform offset: Effects on oceanic crustal and upper mantle structure, *J. Geophys. Res, 93*, 2955–2966.

Plank, T., and C. H. Langmuir (1988), An evaluation of the global variation in the major element chemistry of arc basalts, *Earth Planet. Sci. Lett., 90*, 349–370.

Portnyagin, M., K. Hoernle, G. Avdeiko, F. Hauff, R. Werner, I. Bindeman, V. Uspensky, and D. Garbe-Schonberg (2005), Transition from arc to oceanic magmatism at the Kamchatka-Aleutian junction, *Geology, 33*, 25–28.

Reid, I., and H. R. Jackson (1981), Oceanic spreading rate and crustal thickness, *Mar. Geophys. Res., 5*, 165–172.

Ribe, N. M. (1989), Mantle flow induced by back arc spreading, *Geophys. J. Int., 98*, 85–91.

Ruellan, E., J. Delteil, I. Wright, and T. Matsumoto (2003), From rifting to active spreading in the Lau Basin--Havre Trough backarc system (SW Pacific): Locking/unlocking induced by seamount chain subduction, *Geochem., Geophys., Geosys., 4*, doi: 10.1029/2001GC000261.

Saunders, A. D., and J. Tarney (1979), The geochemistry of basalts from a back-arc spreading center in the East Scotia Sea, *Geochim. Cosmochim. Acta, 43*, 555–572.

Scheirer, D., and K. C. Macdonald (1993), Variation in cross-sectional area of the axial ridge along the East Pacific Rise- Evidence for the magmatic budget of a fast spreading center, *J. Geophys. Res, 98*, 7871–7885.

Schmidt, M. W., and S. Poli (1998), Experimentally based water budgets for dehydrating slabs and consequences for arc magma generation, *Earth Planet. Sci. Lett., 163*, 361–379.

Scholl, D. W., and T. L. Vallier (Eds.) (1985), *Geology and offshore resources of Pacific island arcs; Tonga region*, 488 pp., Circum-Pac. Counc. Energy and Miner. Resour., Houston, TX.

Sclater, J. G., J. W. Hawkins, J. Mammerickx, and C. B. Chase (1972), Crustal extension between the Tonga and Lau ridges: petrologic and geophysical evidence, *Geol. Soc. Am. Bull., 83*, 505–518.

Scott, D. R., and D. J. Stevenson (1989), A self-consistent model of melting, magma migration and buoyancy-driven circulation beneath mid-ocean ridges, *J. Geophys. Res, 94*, 2973–2988.

Sinton, J. M., and P. Fryer (1987), Mariana Trough lavas from 18°N: Implications for the origin of backarc basin basalts, *J. Geophys. Res, 92*, 12782–12802.

Sisson, T. W., and S. Bronto (1998), Evidence for pressure-release melting beneath magmatic arcs from basalt at Galunggung, Indonesia, *Nature*, *391*, 883–886.

Small, C. (1998), Global systematics of mid-ocean ridge morphology, in *Faulting and Magmatism at Mid-Ocean Ridges*, edited by W. R. Buck, et al., pp. 1–25, American Geophysical Union, Washington, D.C.

Smith, W. H. F., and D. T. Sandwell (1997), Global sea floor topography from satellite altimetry and ship depth soundings, *Science*, *277*, 1956–1962.

Sotin, C., and E. M. Parmentier (1989), Dynamical consequences of compositional and thermal density stratification beneath spreading centers, *Geophys. Res. Lett.*, *16*, 835–838.

Spiegelman, M., and D. McKenzie (1987), Simple 2-D models for melt extraction at mid-ocean ridges and island arcs, *Earth Planet. Sci. Lett.*, *83*, 137–152.

Stern, R. J. (2002), Subduction zones, *Rev. Geophys.*, *40*, doi: 10.1029/2001RG000108.

Stern, R. J., S. H. Bloomer, P.-N. Lin, E. Ito, and J. Morris (1988), Shoshonitic magmas in nascent arcs: New evidence from submarine volcanoes in the northern Marianas, *Geology*, *16*, 426–430.

Stern, R. J., E. Kohut, S. H. Bloomer, M. Leybourne, M. Fouch, and J. Vervoort (2006), Subduction factory processes beneath the Guguan cross-chain, Mariana Arc: no role for sediments, are serpentinites important? *Contrib. Mineral. Petrol.*, *151*, 202–221.

Stern, R. J., P.-N. Lin, J. D. Morris, M. C. Jackson, P. Fryer, S. H. Bloomer, and E. Ito (1990), Enriched back-arc basin basalts from the northern Mariana Trough: implications for the magmatic evolution of back-arc basins, *Earth Planet. Sci. Lett.*, *100*, 210–225.

Stern, R. J., N. C. Smoot, and M. Rubin (1984), Unzipping of the Volcano Arc, Japan, *Tectonophysics*, *102*, 153–174.

Stern, T. A. (1987), Asymmetric back-arc spreading, heat flux and structure associated with the Central Volcanic Region of New Zealand, *Earth Planet. Sci. Lett.*, *85*, 265–276.

Stolper, E., and S. Newman (1994), The role of water in the petrogenesis of Mariana trough magmas, *Earth Planet. Sci. Lett.*, *121*, 293–325.

Su, W., and W. R. Buck (1993), Buoyancy effects on mantle flow under mid-ocean ridges, *J. Geophys. Res*, *98*, 12191–12207.

Tamura, Y., Y. Tatsumi, D. Zhao, Y. Kido, and H. Shukuno (2002), Hot fingers in the mantle wedge: new insights into magma genesis in subduction zones, *Earth Planet. Sci. Lett.*, *197*, 105–116.

Tappin, D. R., T. R. Bruns, and E. L. Geist (1994), Rifting of the Tonga/Lau Ridge and formation of the Lau backarc basin: evidence from Site 840 on the Tonga Ridge, in *Proc. ODP Sci. Results*, edited by J. Hawkins, et al., pp. 367–371, Ocean Drilling Program, College Station, TX.

Tarney, J., A. D. Saunders, and S. D. Weaver (1977), Geochemistry of volcanic rocks from the island arcs and marginal basins of the Scotia arc region, in *Island Arcs Deep Sea Trenches and Back-Arc Basins*, edited by M. Talwani and W. C. Pitman III, pp. 367–377, American Geophysical Union, Washington, D.C.

Tatsumi, Y. (1986), Formation of the volcanic front in subduction zones, *Geophys. Res. Lett.*, *13*, 717–720.

Tatsumi, Y., and S. Eggins (1995), *Subduction zone magmatism*, 211 pp., Blackwell Science, Cambridge, Mass., USA.

Taylor, B. (1992), Rifting and the volcanic-tectonic evolution of the Izu-Bonin-Mariana arc, in *Proceedings of the Ocean Drilling Program, Scientific Results, 126*, edited by B. Taylor, et al., pp. 627–651, Ocean Drilling Program, College Station, TX.

Taylor, B., and G. D. Karner (1983), On the evolution of marginal basins, *Reviews of Geophysics Space Phys*, *21*, 1727–1741.

Taylor, B., and F. Martinez (2003), Back-arc basin basalt systematics, *Earth Planet. Sci. Lett.*, *210*, 481–497.

Taylor, B., K. Zellmer, F. Martinez, and A. Goodliffe (1996), Sea-floor spreading in the Lau back-arc basin, *Earth Planet. Sci. Lett.*, *144*, 35–40.

Tiffin, D. L. (1993), GLORIA surveys in frontier areas of the southwest Pacific Ocean, *Geo-Mar. Lett.*, *13*, 65–70.

Turner, I. M., C. Peirce, and M. C. Sinha (1999), Seismic imaging of the axial region of the Valu Fa Ridge, Lau Basin—the accretionary processes of an intermediate back-arc spreading ridge, *Geophys. J. Int.*, *138*, 495–519.

Turner, S., and C. Hawkesworth (1998), Using geochemistry to map mantle flow beneath the Lau Basin, *Geology*, *26*, 1019–1022.

Vallier, T. L., G. A. Jenner, F. A. Frey, J. B. Gill, A. S. Davis, A. M. Volpe, J. W. Hawkins, J. D. Morris, P. A. Carwood, J. L. Morton, D. W. Scholl, M. Rautenschlein, W. M. White, R. W. Williams, A. J. Stevenson, and L. D. White (1991), Subalkaline andesite from Valu Fa Ridge, a back-arc spreading center in southern Lau Basin: petrogenesis, comparative chemistry, and tectonic implications, *Chem. Geol.*, *91*, 227–256.

Volpe, A. M., J. D. Macdougall, G. W. Lugmair, J. W. Hawkins, and P. Lonsdale (1990), Fine-scale isotopic variation in Mariana Trough basalts: evidence for heterogeneity and a recycled component in backarc basin mantle, *Earth Planet. Sci. Lett.*, *100*, 251–264.

Weissel, J. K. (1977), Evolution of the Lau Basin by the growth of small plates, in *Island Arcs, Deep Sea Trenches and Back-Arc Basins*, edited by M. Talwani and W. C. Pitman III, pp. 429–436, American Geophysical Union, Washington, D.C.

Weissel, J. K. (1981), Magnetic lineations in marginal basins of the west Pacific, *Phil. Trans. Roy. Soc. London, Ser. A*, *300*, 223–247.

Wetzel, L. R., D. A. Wiens, and M. C. Kleinrock (1993), Evidence from earthquakes for bookshelf faulting at large non-transform offsets, *Nature*, *362*, 235–237.

Whelan, P. M., J. B. Gill, E. Kollman, R. A. Duncan, and R. E. Drake (1985), Radiometric dating of magmatic stages in Fiji, in *Geology and offshore resources of Pacific island arcs—Tonga region*, edited by D. W. Scholl and T. L. Vallier, pp. 415–440, Circum Pacific Council for Energy and Mineral Resources, Houston, TX.

Wiedicke, M., and J. Collier (1993), Morphology of the Valu Fa Spreading Ridge in the Southern Lau Basin, *J. Geophys. Res*, *98*, 11769–11782.

Wiedicke, M., and W. Habler (1993), Morphotectonic characteristics of a propagating spreading system in the northern Lau Basin, *J. Geophys. Res*, *98*, 11783–11797.

Woodhead, J., S. Eggins, and J. Gamble (1993), High field strength and transition element systematics in island arc and backarc basin basalts: Evidence for multiphase melt extraction and a depleted mantle wedge, *Earth Planet. Sci. Lett.*, *114*, 491–504.

Wright, D. J., S. H. Bloomer, C. J. MacLeod, B. Taylor, and A. M. Goodliffe (2000), Bathymetry of the Tonga trench and forearc: a map series, *Mar. Geophys. Res.*, *21*, 489–511.

Wright, I. C. (1993), Pre-spread rifting and heterogeneous volcanism in the southern Havre Trough back-arc basin, *Marine Geol.*, *113*, 179–200.

Wright, I. C., L. M. Parson, and J. A. Gamble (1996), Evolution and interaction of migrating cross arc volcanism and back-arc rifting: An example from the southern Havre Trough (35°20′–37°S), *J. Geophys. Res*, *101*, 22,071–022,086.

Yamazaki, T., and F. Murakami (1998), Asymmetric rifting of the northern Mariana Trough, *The Island Arc*, *7*, 460–470.

Yamazaki, T., N. Seama, K. Okino, K. Kitada, M. Joshima, H. Oda, and J. Naka (2003), Spreading process of the northern Mariana Trough: Rifting-spreading transition at 22°N, *Geochem. Geophys. Geosyst.*, *4*, DOI 10.1029/2002GC000492.

Zellmer, K. E., and B. Taylor (2001), A three-plate kinematic model for Lau Basin opening, *Geochem. Geophys. Geosyst.*, *2*, 2000GC000106.

Fernando Martinez and Brian Taylor, School of Ocean and Earth Science and Technology, University of Hawaii at Manoa, 1680 East West Road, Honolulu, Hawaii, USA. (fernando@hawaii.edu)